RING & SECTOR ANALYSIS, AND SITE 'IT' ON GREENLAND*

DICK STAPERT
Vakgroep Archeologie, Groningen, Netherlands

LYKKE JOHANSEN
Institut for Arkæologi og Etnologi, København, Denmark

ABSTRACT: A technique for applying the ring and sector method to grid-cell data is introduced. In cases where the cells are not larger than 50x50 cm, it is possible to adjust for distortions ('pseudo-peaks') created by the artefacts from the sieve having artificial coordinates in the centres of the cells. This is achieved by comparing the observed ring (or sector) distributions with those produced on the basis of a theoretical test file reflecting randomness. The procedure is tested and illustrated, using mainly the data of an early Dorset site on Greenland ('IT'). The outcomes of the ring and sector analysis are contrasted with the results of a refitting analysis of the same site. The main subject of the paper is the use of ring and sector analysis for establishing the presence of dwelling structures, independently of archaeologically visible features.

KEYWORDS: Intrasite spatial analysis, ring and sector method, grid-cell data, dwelling structures, Upper/Late Palaeolithic in Europe, Dorset Culture in Greenland.

1. INTRODUCTION

The ring and sector method was developed for intrasite spatial analysis of Stone Age sites with a central hearth (Stapert, 1990; 1992). Around the centre of the hearth a system of rings and sectors is positioned, and the frequencies of artefacts in the rings and sectors are counted per class. One of the main contributions of the method is that, in many cases, it may reveal whether a hearth was located inside a dwelling or in the open air. Unimodal ring distributions were found to be characteristic of outdoor hearths, while multimodal ring distributions (showing two or three peaks) are associated with hearths inside dwellings. In this paper, the ring and sector approach is critically evaluated, partly prompted by the review by De Bie (1993), and partly as a result of our analysis of the 'IT' site on Greenland. IT is an early Dorset site in the Disko Bay area of western Greenland, where several dwelling structures with central hearths have been excavated (see under 6).

A computer program for executing ring and sector analysis has been developed by Akili Software in Groningen; it operates with Cartesian coordinates (Boekschoten & Stapert, 1993; in press). The program makes it possible to explore the ring and sector method in depth. Among other things, it allows the optimum level of resolution for any site to be established, which is a prerequisite for meaningful quantitative approaches in spatial analysis. In this paper it is shown that the quest for an appropriate measuring scale is of crucial importance especially in applying the ring approach.

One of the main topics of our work was to develop ways to perform ring analysis in the case of sites where part of the material was collected per quarter square metre. At many modern excavations the excavated soil is sieved per quarter square metre. In the case of the IT site, sieving was precluded because of the nature of the soil (peat). All excavated soil was carefully sorted through by hand on a table, per quarter square metre. However, tools and larger artefacts were measured in individually. Up till now, the ring and sector method was mostly applied only to artefacts with individual coordinates, which of course is the most reliable approach. However, this also implies a serious restriction. It is unsatisfactory that only part of the available evidence is used in the analysis. Using grid-cell data is possible only if the method is adapted to that situation, and this paper is an attempt to do just that. This seemed very important to us, because it would make the method applicable even at sites where the bulk of the material was collected in grid cells. In the case of IT, of the total of 15,980 artefacts, only 596 have exact coordinates: 3.7%. The rest were collected by the quarter square metre in the way described above. This situation makes it very clear that we need reliable procedures to cope with grid-cell data. We believe that the methods developed in this paper will prove to be a step in the right direction. If they do, the scope and usefulness of the ring and sector method will be greatly enhanced.

* The computer drawings in this paper, by Dick Stapert, were made using both 'Rings & Sectors' and 'SlideWrite Plus'.

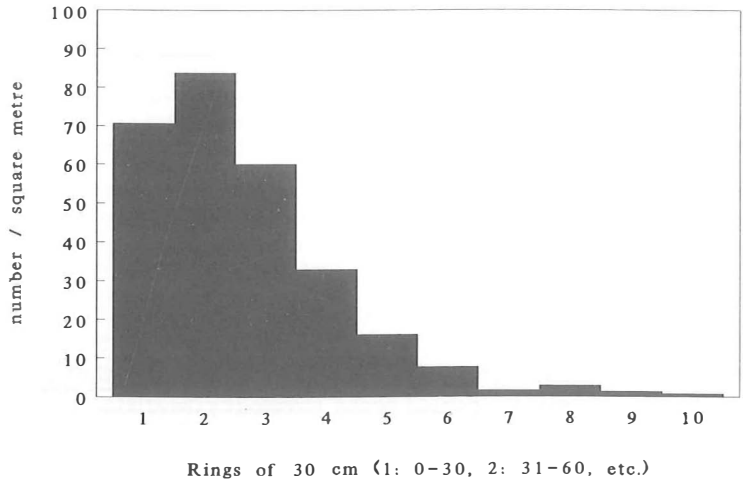

Fig. 1. Pincevent T112. Tools in rings of 30 cm, expressed as densities: number/square metre. In all ring diagrams in this paper, the X-axis indicates the distance to the hearth centre. N = 334.

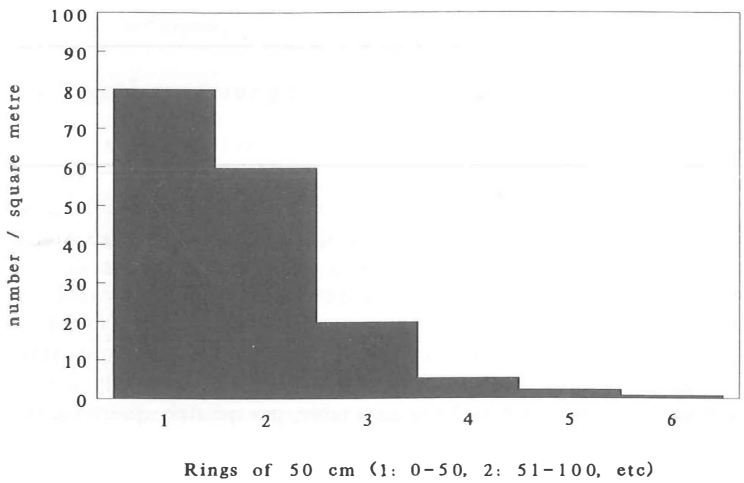

Fig. 2. Pincevent T112. Tools in rings of 50 cm, expressed as densities: number/square metre.

2. RING ANALYSIS AS A ONE-DIMENSIONAL APPROACH

Up till now, ring analysis was performed by counting the actual frequencies in the rings, per artefact group, and presenting these in the form of histograms (Stapert, 1992). In most cases, rings of 0.5 m were employed. Several commentators (e.g. Blankholm, 1991/92; De Bie, 1993; E. Cziesla, pers. comm. 1989; L.P. Louwe Kooijmans, pers. comm. 1992) have expressed some amazement at this procedure. Since the rings grow (linearly) in surface area, going outwards from the centre, it might seem more logical to transform the ring frequencies into densities, i.e. numbers per square metre. The first author has always avoided this transformation, for several reasons (see Stapert, 1989: p. 7). The most important of these is the realization that ring data are *distance* data. In other words, we may regard ring analysis as a one-dimensional approach. Therefore, it would perhaps be more precise not to speak of rings, but of *distance classes*. One may imagine a single prehistoric activity, for example the production of an antler spearhead, for which five burins were used. These would always be the same five burins, irrespective of whether the work was done close to the hearth or at a large distance. We are interested in the distance to the hearth of these five burins, not in the averaged density of these tools, calculated for a complete ring. Ring densities would create the false impression that tools are scattered evenly in the rings, which is not the case. Therefore, this transformation seemed superfluous and in some cases even misleading. Density patterns are more usefully studied in a grid, preferably with cells of 50x50 cm.

However, transforming ring frequencies into ring densities is not without value altogether. This procedure may convey information about global density patterns in relation to the hearth. In most cases, it can be shown in this way that the hearth is associated with high densities in the artefact scatter. In a paper on Pincevent (France), a ring density diagram for the tools at Concentration T112 was included, for comparison with

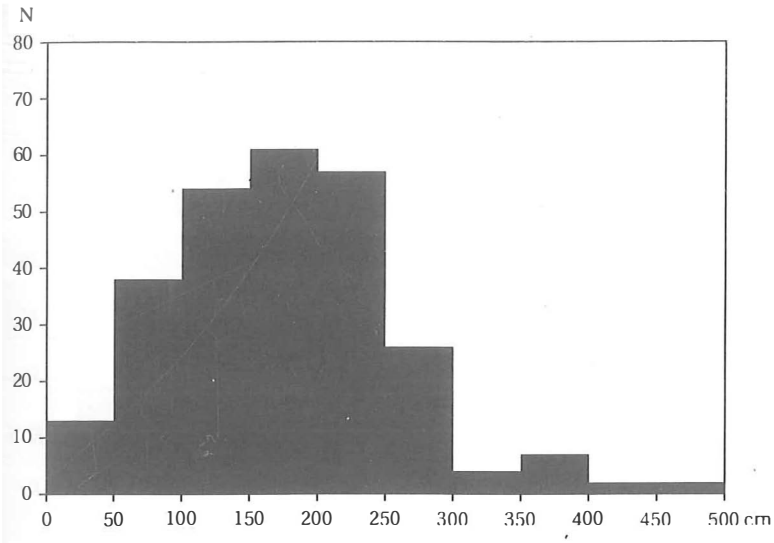

Fig. 3. Oldeholtwolde. Tools (including broken-off borer-tips) in rings of 50 cm: frequencies. N = 264; mean D: 1.75 m.

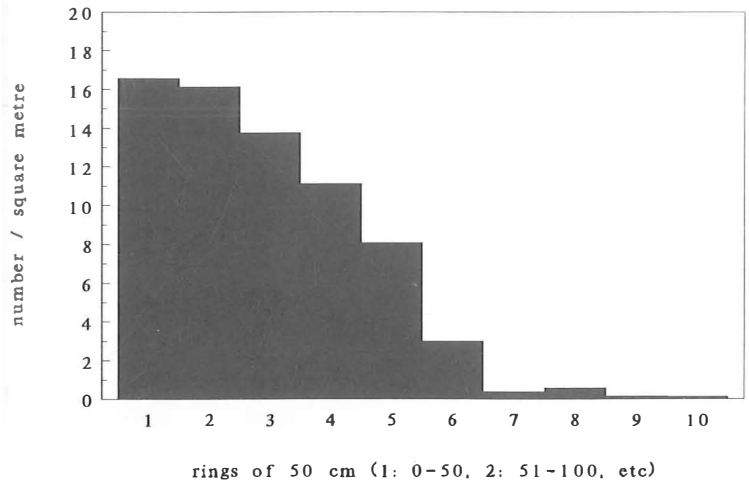

Fig. 4. Oldeholtwolde. Same data as in fig. 3, now expressed as densities: number/square metre.

an 'ordinary' ring diagram showing frequencies per ring (Stapert, 1989: figs 2 and 16, respectively). Density diagrams are illustrated here again for Pincevent T112, using rings of 30 cm and 50 cm (figs 1 and 2; compare these figures with figs 9 and 10, in which the frequencies using the same ring widths are given). Note that the mode in the density diagrams is closer to the centre than in the frequency diagrams. In the case of rings 50 cm wide, the mode of the density diagram even falls in the first ring. The same difference can be observed, even more markedly, in figures 3 and 4, which show a frequency diagram and a density diagram for the tools of the Hamburgian site at Oldeholtwolde (the Netherlands), using ten rings of 50 cm. The density diagram very clearly shows the 'central tendency': the association of the hearth with high density. The highest density occurs in the first ring, 0-50 cm from the hearth centre. In terms of frequency, there are only 13 tools in this ring. In the ring with the highest number of tools, between 1.5 and 2 m, there are 61 tools – almost five times as many. The point, illustrated by figure 3, is that it is clearly at some distance from the hearth, between about 1 and 2.5 m from its centre, that most activities involving the use of tools were performed – not very close to, or even within the hearth, as the density diagram seems to suggest. In other words, it is the frequency diagram that shows where activities were really going on. The density diagram expresses something else. It shows that, globally speaking, the hearth was indeed the focus of the artefact scatter under discussion, but not much more.

A nasty consequence of transforming ring frequencies to densities is that the patterns we wish to study become blurred. With increasing distance from the hearth, patterns evident in the ring distributions will become less and less visible, because the ring frequencies have to be divided by ever larger surface areas. Fluctuations in ring frequencies are thus more and more suppressed and marginalized as we move outwards from the hearth.

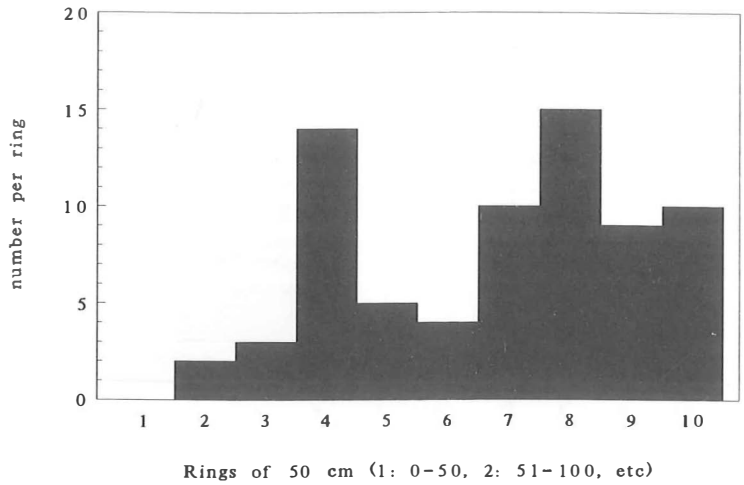

Fig. 5. Gönnersdorf II. Backed bladelets in the NW quarter in rings of 50 cm: frequencies. N = 72.

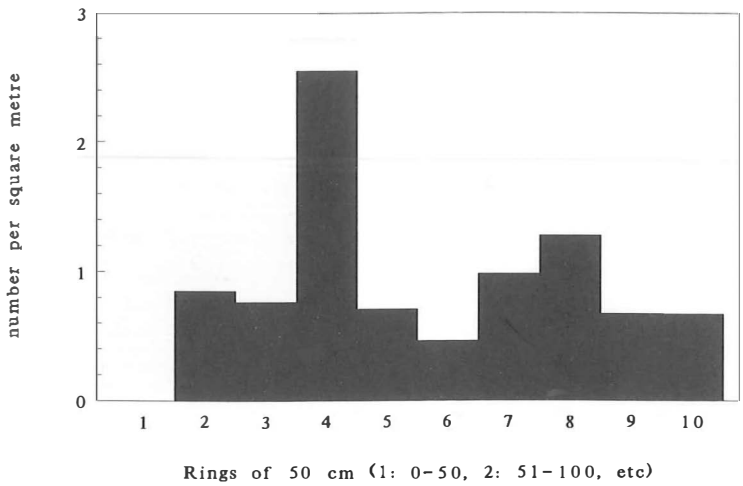

Fig. 6. Gönnersdorf II. Same data as in fig. 5, now expressed as densities: number/square metre.

This is a problem especially with multimodal ring distributions. As an example, the frequency diagram for backed bladelets in the northwestern quarter of Concentration II at Gönnersdorf (Germany) is shown in figure 5 (see Boekschoten & Stapert, 1993: fig. 5A). In this diagram, a second peak between 3.5 and 4 m is very conspicuous. Transforming the data to densities results in the diagram shown in figure 6. The bimodal pattern is not lost, but it has become much less prominent. In the frequency diagram the second peak is about as high as the first (n = 15 and 14, respectively); in the density diagram the second mode is only half as high as the first (n/sq.m. = 2.55 and 1.27, respectively). This is solely the result of the growing surface areas of the rings. If the second peak in the frequency diagram had been lower, it could have disappeared completely in the density diagram. Transforming the data shows that the second peak, caused by the barrier effect of the tent wall, is a modest phenomenon in terms of density. Nevertheless, it is a remarkable phenomenon in the frequency diagram. It is also a very useful phenomenon, because it can be interpreted, so there seems little reason to obscure it. The answer probably is that De Bie (and others) felt that using densities is more 'honest' than using frequencies. In our opinion, however, it is perfectly legitimate to consider ring analysis as a one-dimensional approach.

There is one aspect of the growing rings, however, which merits closer consideration. The surface areas of the rings may, to a certain degree, be used to investigate whether or not patterns observed in ring diagrams could be a product of chance. We shall return to this possibility in later sections of this paper.

3. SEARCHING FOR THE OPTIMUM LEVEL OF RESOLUTION

The use of histograms to present distance data has several weaknesses. As De Bie (1993: p. 139) rightly remarked, their shape is partly dependent on the selected ring width. This problem has two important aspects:

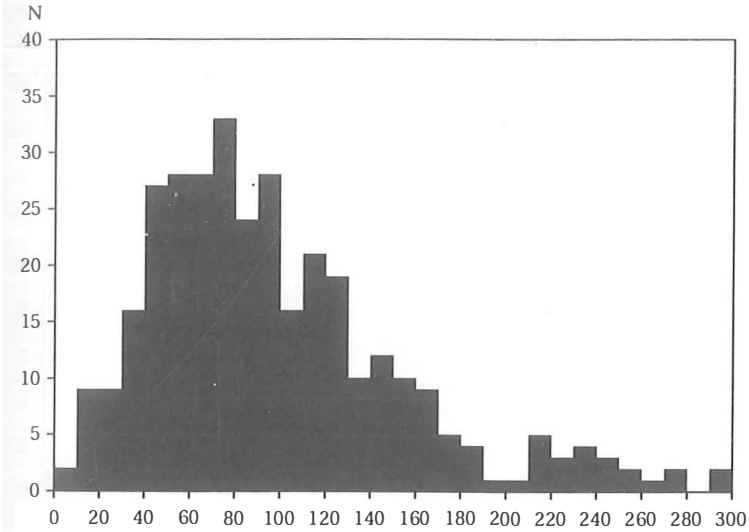

Fig. 7. Pincevent Tl 12. Tools in rings of 10 cm. N = 334; mean D: 0.98 m.

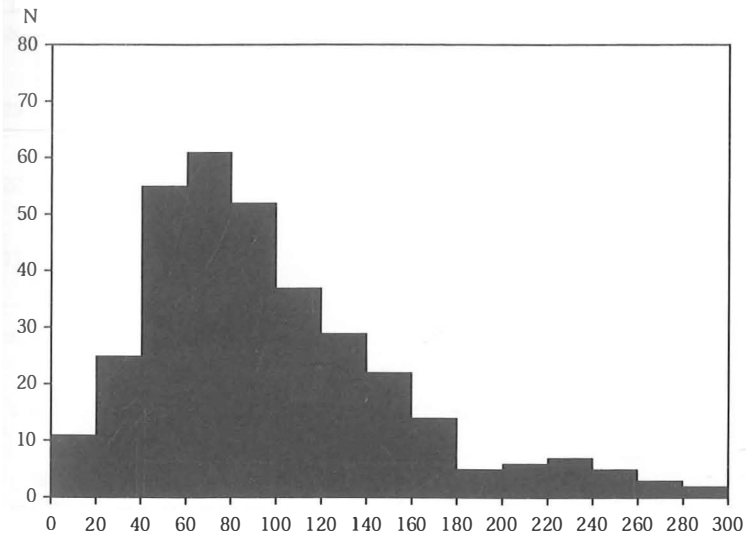

Fig. 8. Pincevent T112. Tools in rings of 20 cm.

reliability and precision. In other words, we are confronted with the search for the optimum level of resolution. Throughout the thesis of the first author (Stapert, 1992), rings of 0.5 m were employed. A computer program was not available at that time, and all the measurements and subsequent data manipulation were done by hand. Since then, the computer package 'RINGS & SECTORS' (R&S for short) has been developed (Boekschoten & Stapert, 1993; in press). One of the main advantages of a program such as R&S is that it enables the user to 'play about' with spatial data. This possibility of playing does not necessarily imply improper manipulation of the data. The goal is to find structure in the data jungle; playing is part of the pattern-recognition process. Most patterns, including those displayed by distance data, are not indifferent to scale. Therefore, one has to find the optimum parameters for each site under analysis. In other words, one has to 'focus' any method for spatial analysis, by establishing the optimum level of resolution in each case (Boekschoten et al., 1994).

Finding the optimum level of resolution is a basic problem in any quantitative science. This quest is an interplay between the wish to preserve and use as much information as possible and the need for statistical reliability. The more artefacts, the finer our measuring scales can be. Using too narrow rings may lead to fragmentation of the data, and the histogram will then show many irregularities. Using too wide rings could easily obscure the patterns we are looking for. For example, when dealing with a dwelling structure with a diameter of less than 5 m, rings of 0.5 m may in some cases be too wide for bringing out the position of the walls. One would need narrower rings in such cases (40 or 30 cm, or even less), but this makes sense only if there are enough artefacts. If their number is too small,

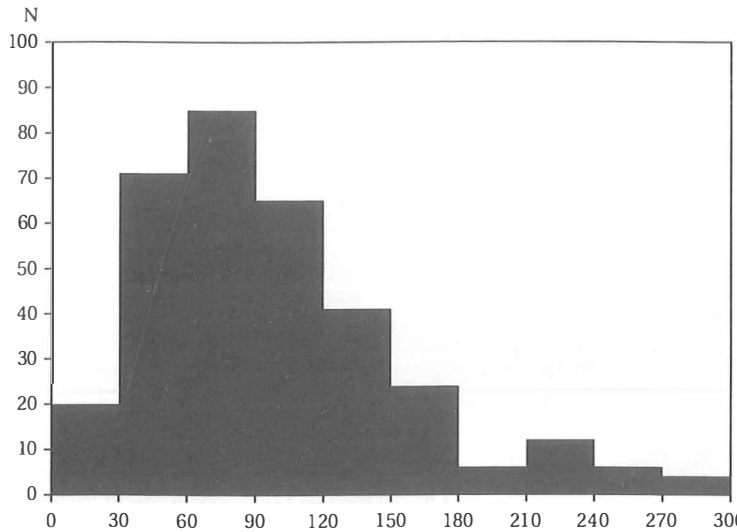

Fig. 9. Pincevent T112. Tools in rings of 30 cm.

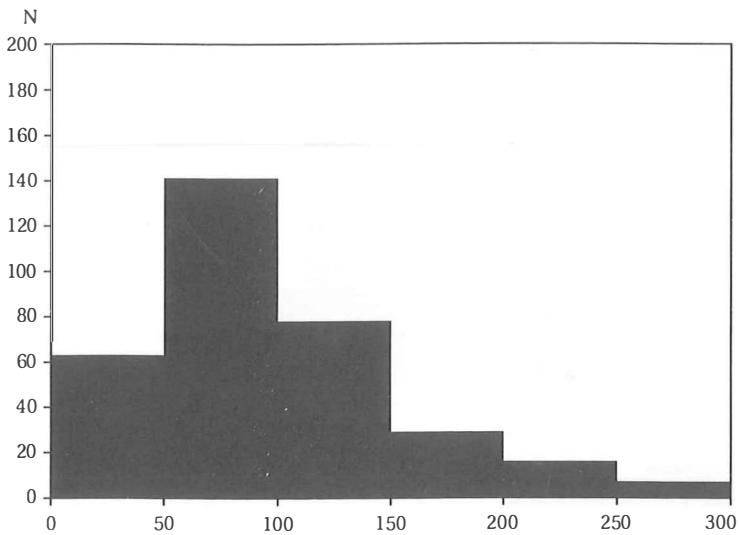

Fig. 10. Pincevent T112. Tools in rings of 50 cm.

any structures could remain undetectable to the ring and sector method. The R&S program makes it possible to explore the whole scale of measurement, from fine to coarse, and to establish the scale that is appropriate for any individual site. To illustrate this search, ring diagrams for the tools of Pincevent T112 are shown, using rings of 10, 20, 30 and 50 cm (figs 7-10). In the case of rings 10 cm wide (fig. 7), the curve shows many irregularities. The graph has not 'stabilized', because the measuring scale is too fine-grained. By virtue of the large number of tools (334 within 3 m from the hearth centre), the graph has already stabilized when rings of 20 cm are used (fig. 8). With 10 rings of 30 cm, still a clear picture is obtained (fig. 9). In the case of 50-cm rings (fig. 10), the graph is somewhat too coarse-grained. For example, the small peak between 2 and 2.5 m, visible in figures 8 and 9, is now lost. In the case of Pincevent T112, because of the large number of tools, the use of rings 25 cm wide would probably be the best choice.

Large tents, such as those of Gönnersdorf, are clearly visible when rings of 50 cm are used (see fig. 5). As noted above, finding the optimum level of resolution is especially important when we are dealing with relatively small dwellings. This is illustrated here by the case of Andernach-Oben (Germany), the *Federmesser* site stratigraphically overlying the well-known Magdalenian site at Andernach-Martinsberg. The data were kindly made available to us by Dr Martin Street (Forschungsstelle Monrepos, Neuwied). In figures 11-15, only the artefacts that were measured in individually have been taken into account. At this site, Street identified three hearths, on the basis of dense concentrations of burnt bone. The westernmost one, hearth A, is associated with nine different raw materials, both local and exogenous. In figures 11-15, the artefacts of these raw materials,

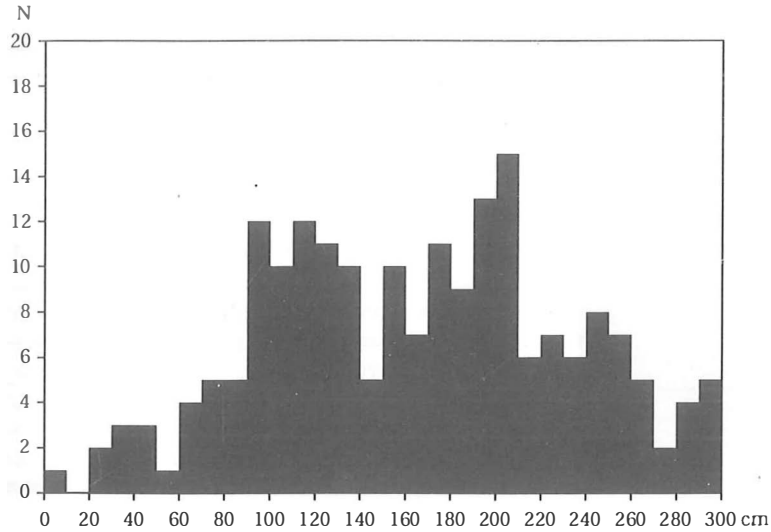

Fig. 11. Andernach-Oben. Artefacts of nine raw materials in rings of 10 cm around the centre of Hearth A (coordinates: 19.0/86.5). N = 199.

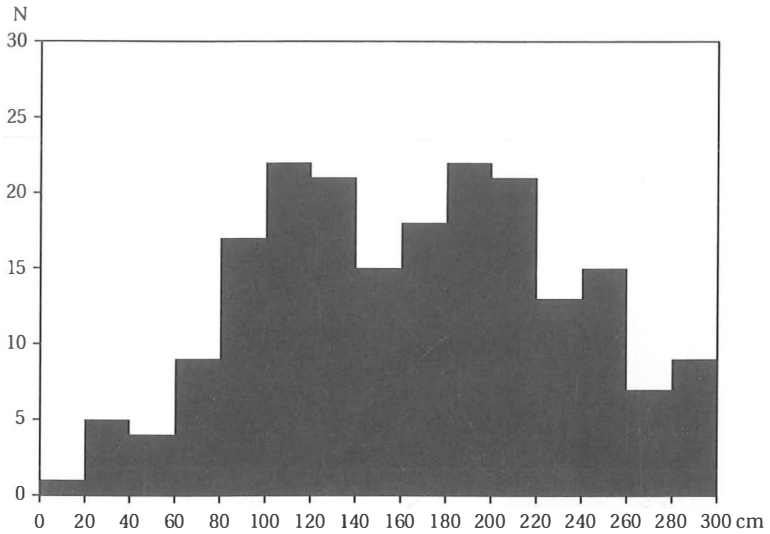

Fig. 12. Andernach-Oben. The same artefacts as in fig. 11, now in rings of 20 cm.

both tools and non-tools, are presented in rings of 10, 20, 30, 40 and 50 cm width. Though the diagram for rings of 20 cm already shows bimodality, there are still some irregularities. With rings of 30 cm the graph is stabilized. It is bimodal with the second mode between 1.8 and 2.1 m, suggesting the presence of a tent or hut with a diameter of about 4 m. In the diagram using rings of 40 cm, bimodality has become all but invisible. In the case of rings 50 cm wide, the graph has changed into a unimodal histogram, and the bimodality which is evident when we use smaller rings has been lost. Using the same procedure, tents with diameters of about 4 m can be demonstrated at three units at the Magdalenian site of Marsangy (France): H17, D14 and X18. For the first two of these, Schmider (e.g. 1993) had postulated tents with diameters of 3 to 3.5 m.

Tents with diameters below about 3.5 m will be difficult to detect by the ring and sector method, especially if the numbers of artefacts are relatively small. The two modes will then overlap, because they are so close together. Such situations might result in just a single relatively wide mode, unless very narrow rings could be employed. On the other hand, small tents – with diameters less than about 3 m – would not be expected to have an interior hearth, for lack of space. Buschkämper (1993) analysed two structures at Gönnersdorf (SW1 and SW2), consisting of stone rings with diameters of 2 to 2.5 m, and interpreted them as tent rings. There were no hearths within these rings, and Bussˇkämper therefore did not expect bimodal ring distributions. The centre of the ring and sector system was placed at the geometrical centre of the stone rings. He hypothesized unimodal ring diagrams in such cases, in which the only mode would roughly coincide with the tent walls. He used rings of 25 cm, and indeed found only one peak, indicating the location of the walls.

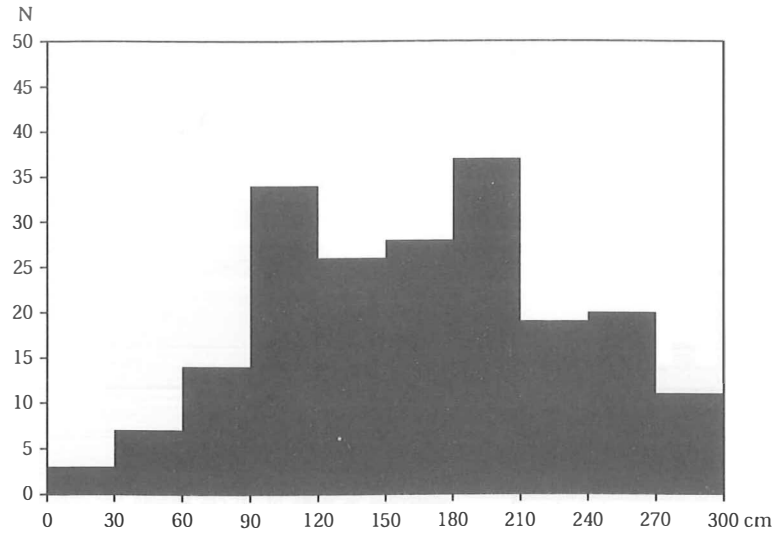

Fig. 13. Andernach-Oben. The same artefacts as in fig. 11, now in rings of 30 cm.

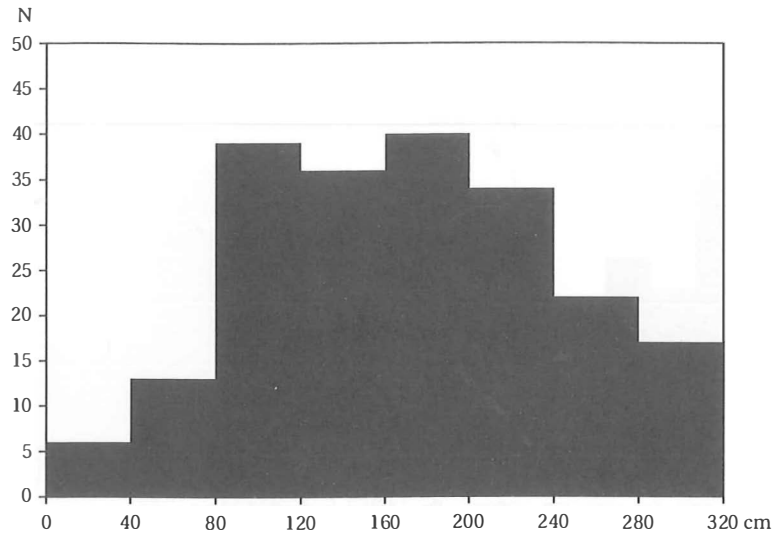

Fig. 14. Andernach-Oben. The same artefacts as in fig. 11, now in rings of 40 cm.

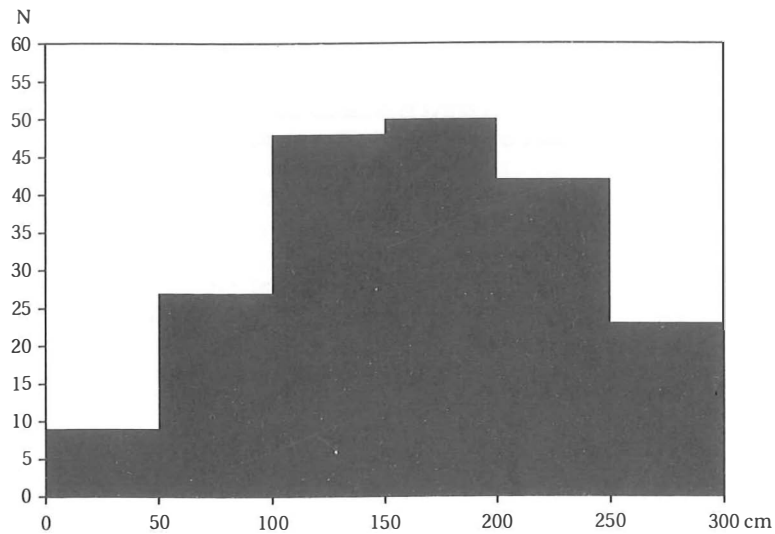

Fig. 15. Andernach-Oben. The same artefacts as in fig. 11, now in rings of 50 cm.

Naturally, finding the optimum level of resolution is also important in sector analysis: the more artefacts, the more sectors can be employed.

4. TRACE LINES

Finding the optimum level of resolution for ring histograms can be done by going through the whole scale of measurement, from narrow to wide rings, and establishing the smallest ring width at which the graph stabilizes. Even then, however, class boundaries remain somewhat arbitrary. An alternative way of analysing distance data is the trace line or ogive. This is a cumulative frequency graph. The artefacts are ranked according to their distance from the hearth centre. In the bottom left corner of the graph, the artefact closest to the hearth is plotted; in the top right corner the farthest one. 'An ogive takes the form of a graph with the values on the horizontal axis representing the stated value and all values below. The vertical axis can be scaled in frequencies or percentages (or both). Ogives can be used for grouped data and for actual values of continuous data.' (Fletcher & Lock, 1991: p. 27). In the R&S program, the actual values are shown in the graph as dots. On the Y-axis, either frequencies or percentages can be indicated. The dots may or may not be connected by a line. It is possible to place a grid over the diagram, so that interesting spots in the graph can easily be located on both axes.

This procedure results in characteristically S-shaped trace lines for artefact scatters around open-air hearths. The steep part in the curve reflects the only peak in the corresponding unimodal histogram: the drop zone. In figure 16, the trace line for the tools of Pincevent T112 is given (compare with figs 7-10), and figure 17 shows the trace line for the tools of Oldeholtwolde (compare with fig. 3). At sites with a hearth inside a dwelling

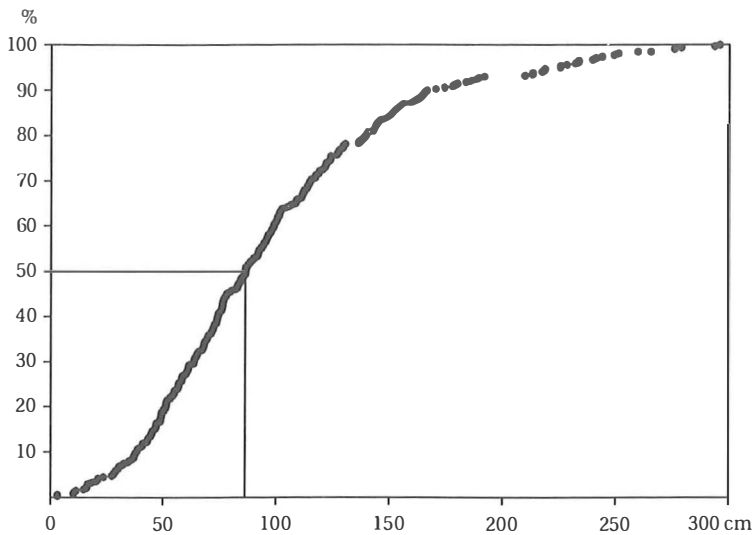

Fig. 16. Pincevent T112. Trace line for the tools. The X-axis indicates the distance to the hearth centre. On the Y-axis, the frequencies are expressed as percentages. N = 334. The median (0.86 m) is indicated in the figure.

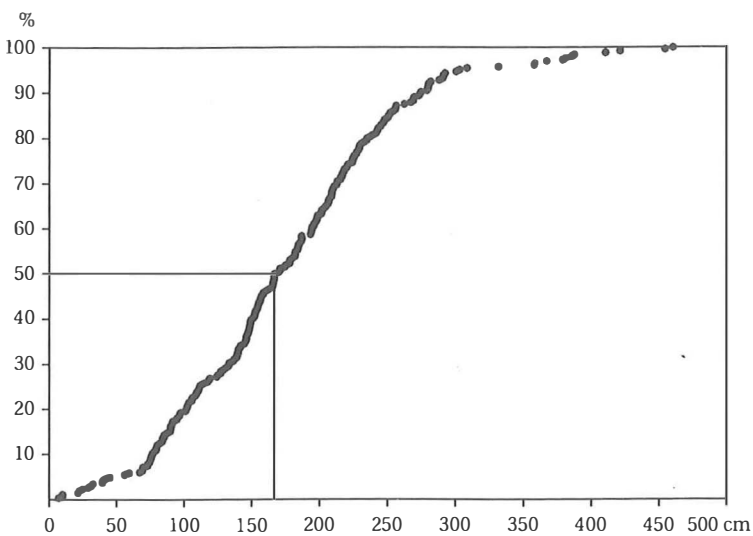

Fig. 17. Oldeholtwolde. Trace line for the tools, including broken-off borer-tips. N = 264. Median: 1.67 m.

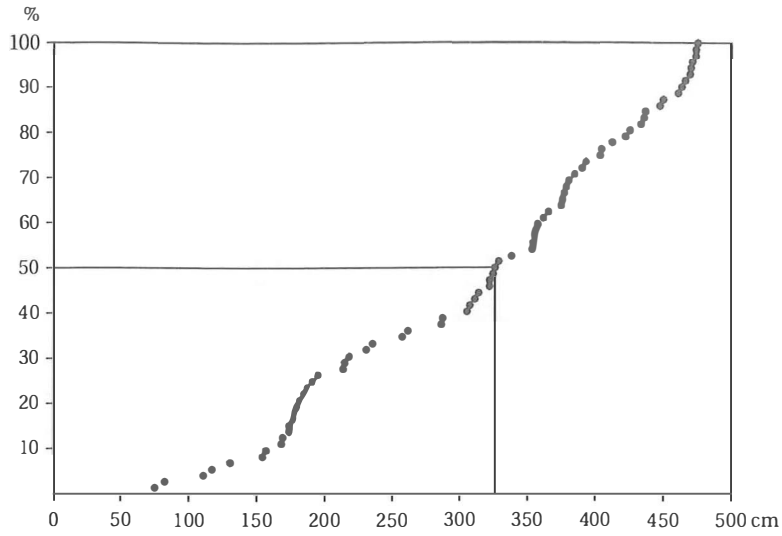

Fig. 18. Gönnersdorf II. Trace line for the backed bladelets in the NW quarter. N = 72. Median: 3.26 m.

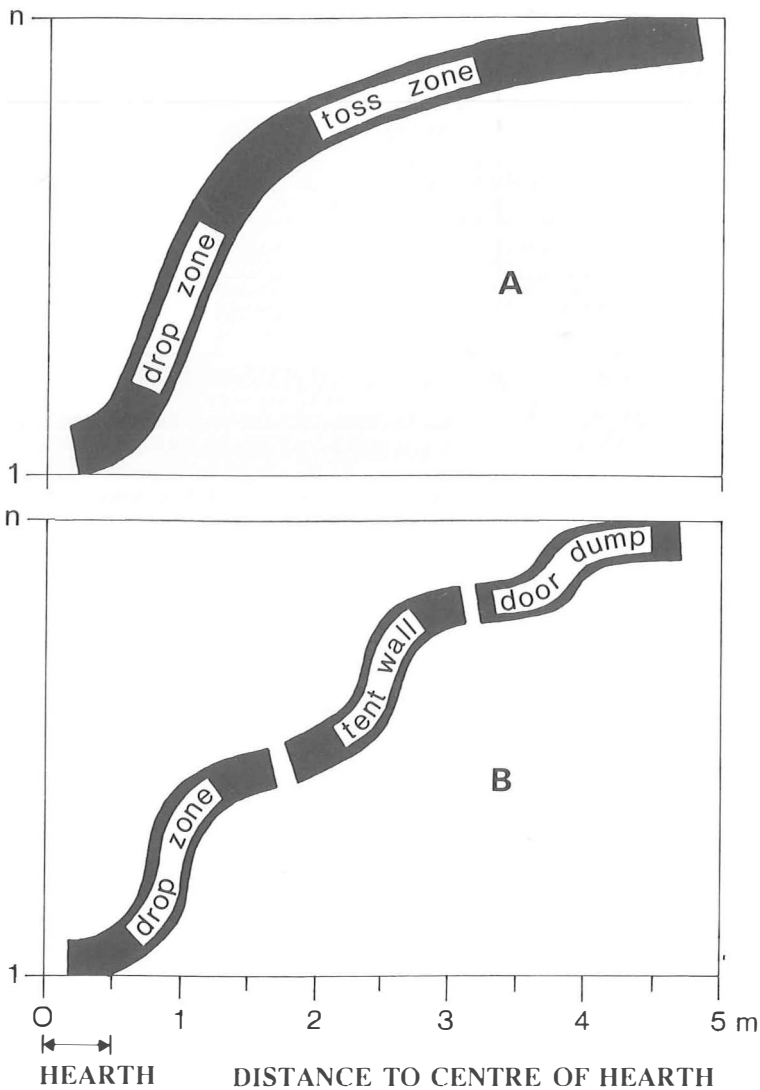

Fig. 19. Diagram showing the global shape of trace lines in the cases of open-air hearths (A) and hearths insidedwellings (B). Drawing Dick Stapert/Lykke Johansen.

structure, two or three S-shaped sections will be observed in the trace line. As an example, the trace line for the backed bladelets in the northwestern quarter of Gönnersdorf II is given (fig. 18; compare with fig. 5). The first 'S' reflects the drop zone. The second is caused by the tent wall, which will have been located just beyond the end of the steep part. A third S-shaped section, if present, may represent a door dump outside the entrance. For a schematic impression of what trace lines will look like for unimodal and multimodal ring distributions, see figure 19. The advantage of trace lines over ring diagrams (histograms) is that no class division is needed. Therefore it is more precise in establishing the position of the tent wall, especially when trace lines are produced for 4 or 8 sectors rather than for the site as a whole.

Note that trace lines illustrate the one-dimensional approach in distance analysis; they are equivalent to frequency histograms.

5. GROWING RINGS

Though ring analysis can be considered a one-dimensional approach, it nevertheless remains true that the artefacts, and the rings, are located in two-dimensional space. It is important to be aware of this during the analysis, for example in situations where some rings are incomplete (because they partly extend outside the excavation borders). However, this is not a crucial problem, because in such cases both frequencies and densities will be affected. Moreover, it is possible to some degree to 'compensate' for partial rings (Stapert & Terberger, 1989; see also under 8). When using frequencies, we do not take into account at all the fact that the rings grow in surface area, going outwards from the hearth. There is one reason, however, to look also at our data in a two-dimensional way: it may be useful to know how much any observed ring distribution deviates from a random (or regular) distribution. To accomplish this, we can produce a histogram showing the surface areas of the rings we use in our analysis (they grow linearly), and compare this theoretical distribution with the observed distribution. To do this, the Y-axis has to be standardized, i.e. transformed into percentages. When ten rings are used (of whatever width), the surface areas of the rings, expressed as percentages of the total area, grow in the way illustrated in figure 20. This figure also represents what we would expect a ring distribution to look like for a site where the artefacts are scattered in a random (or regular) way. Comparison with any observed distribution will show in which rings the actual ring frequencies are higher or lower than would be expected in the case of a random scatter (randomness is here approximated by a regular spatial distribution). This procedure was followed in the case of Gönnersdorf III (Stapert & Terberger, 1989: fig 14). Note that the theoretical distribution can be corrected for missing ring parts. The same procedure is illustrated here for Concentration T112 of Pincevent (fig. 21). It is immediately clear from this graph that up to 1.5 m from the hearth centre, ring percentages are higher than would be expected if the artefacts within 3 m from the hearth centre were scattered randomly or regularly. Beyond 1.5 m, the observed percentages fall below those of the theoretical graph.

The information contained in figure 21 can also be presented in another way, which is perhaps more transparent. For any observed distribution, we can calculate the deviations from the theoretical curve, positive or negative, and present these in a diagram, in which zero on the Y-axis represents the ring percentage of the theoretical distribution reflecting randomness. The resulting graphs for Pincevent T112 and Oldeholtwolde are shown in figures 22 and 23. The two graphs are similar in shape, but note that different ring widths were used; the crossing of the zero-line at Pincevent occurs at 1.5 m, at Oldeholtwolde at 2.5 m. The backed

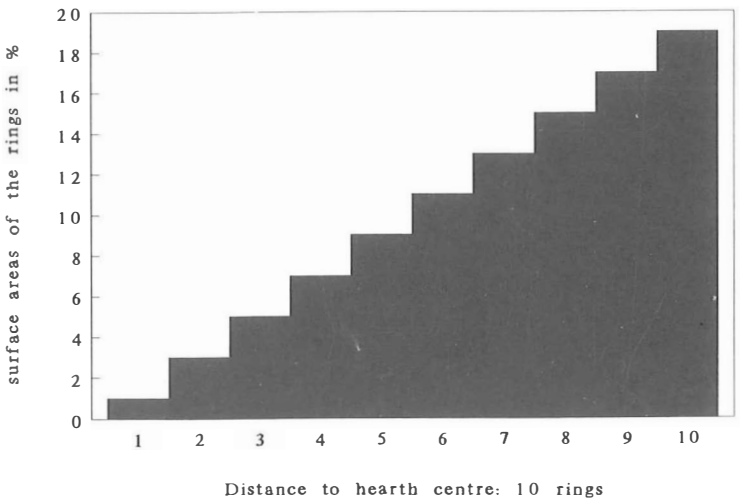

Fig. 20. Surface areas of 10 rings, expressed as percentages of the total area on the Y-axis.

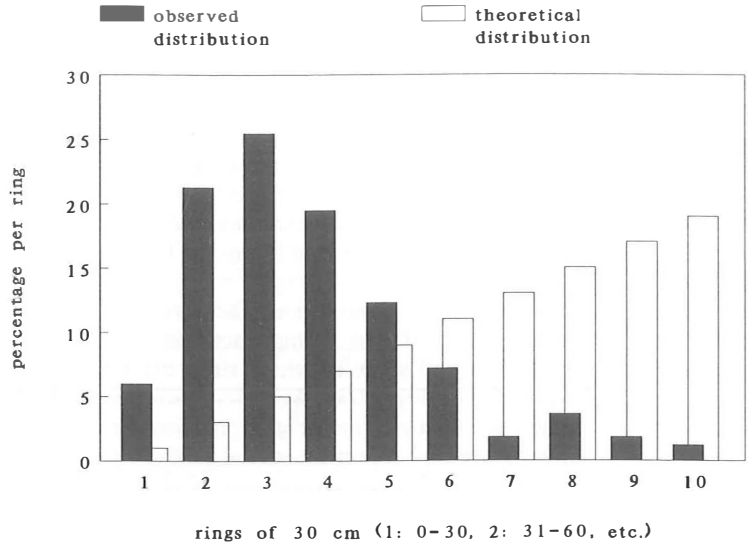

Fig. 21. Pincevent T112. Observed ring distribution of the tools in rings of 30 cm, expressed as percentages on the Y-axis, contrasted with the theoretical distribution of fig. 20 for random or regular spatial scatters.

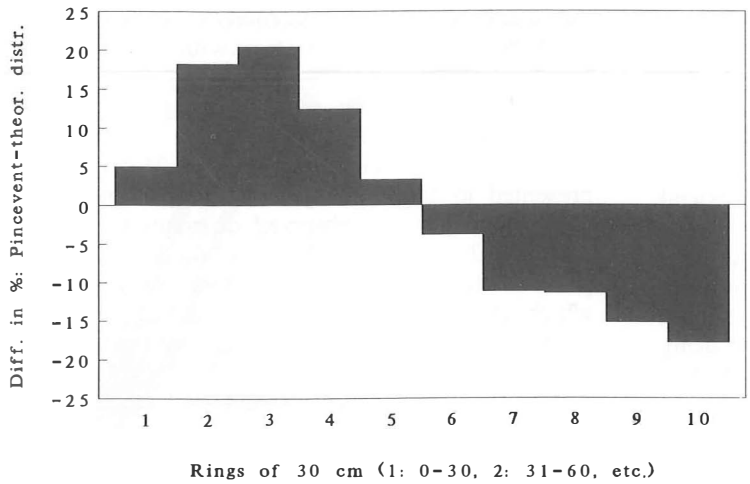

Fig. 22. Pincevent T112. The same data as in fig. 21, but now the deviations from the theoretical curve, as displayed by the observed distribution, are given in percentages on the Y-axis. This curve is more transparent than that of fig. 21.

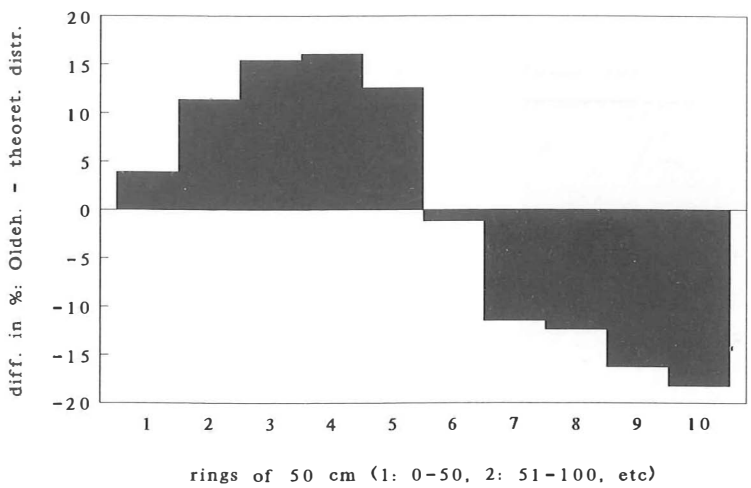

Fig. 23. Oldeholtwolde. Deviations from the theoretical curve of fig. 20, displayed by the observed distribution, are given in percentages on the Y-axis. Rings of 50 cm.

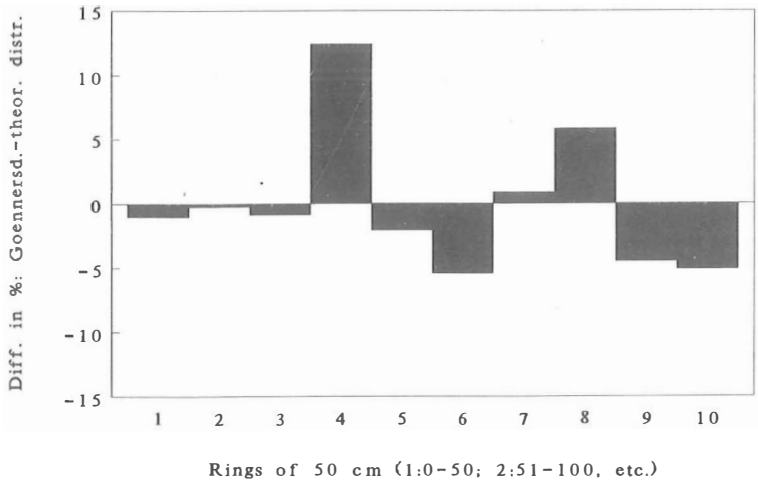

Fig. 24. Gönnersdorf II. Deviations from the theoretical curve of fig. 20, displayed by the observed distribution of the backed bladelets in the NW quarter, are given in percentages on the Y-axis. Rings of 50 cm.

blades in the NW quarter of Gönnersdorf show a very different type of graph (fig. 24). The drop zone near the hearth, and the second peak – reflecting the barrier effect of the tent wall – clearly show up. The tent wall in this quarter will have been located at about 4 m from the hearth centre. This type of diagram will be explored in this paper for the analysis of the IT site on Greenland. The reason for this exercise is not only the wish to investigate to what degree observed ring distributions could be the result of chance (randomness). There is a more practical reason as well, which is to make it possible to use the ring method in cases where most of the material was collected per quarter sq.m.

Note that the method proposed here is not another way of transforming distance data to densities. Ring frequencies are not divided by surface areas; instead, the latter are subtracted from the frequencies (both expressed as percentages). Note also that the shape of the resulting curve is partly dependent on the area covered by the analysis.

6. IKKARLUSSUUP TIMA ('IT')

Ikkarlussuup Tima, hereafter called 'IT', is an early Dorset site (first millennium BC) in Disko Bay, Western Greenland. It was excavated in the summer of 1993 for Aasiaat Museum (Greenland), by a team from Aasiaat Museum, the Memorial University of St. John's (Canada) and the University of Copenhagen (Denmark). The second author took part in the excavation and together with another participant, Erik Brinch Petersen (Copenhagen), she completed a classification of the material. She also produced the data file under the format of R&S, and performed a refitting analysis of the lithic material at IT (see section 12). In 1995 and 1996, further excavation at IT took place, the results of which are not considered in this paper.

The site is located on a raised beach (1.5 m) on the outermost tip of the Nuuk Peninsula. The excavated area is on a cobble beach, which sometimes made it difficult to distinguish between stones occurring naturally and stones incorporated in man-made constructions. In total, some 16,000 artefacts were excavated at IT (fig. 25). About 13,000 of these are chips: pieces smaller than 1 cm.

Three main structures have been recognized (fig. 26). In the southern part of the excavated area a platform, or stone pavement, was present. The stones used to build the platform all derive from the nearby rocks. Around the platform there was a rather indistinct and partial tent ring (not indicated in fig. 26), constructed of stones larger than those occurring naturally on the beach. Inside the tent ring there were three hearths, of which at least one must have been contemporaneous with the tent ring, because it was located centrally. The two other hearths might be of a later date. The entrance of the tent probably faced north, because there seems to be a door dump in that area. At the southern periphery of the tent ring there was a meat-cache, probably contemporaneous with the tent ring.

In the northeastern part of the excavated area another tent ring was excavated. It had a clear ring of large stones around a central hearth, which was built in a small depression and paved with large slabs. In the northern part of this tent ring there was a raised sleeping platform. Outside the tent ring, to the west, there was a rather disturbed meat-cache, which might have belonged to the tent.

In the middle of the northern part of the excavated terrain a large dwelling structure was excavated, interpreted during excavation as a sod house. An outer ring of stones was very distinct in the eastern half, but less clear in the west. An inner ring of stones also seems to be present but is less clear than the outer ring. The central hearth was constructed in a small depression, but without a stone pavement; it was filled with burnt blubber and burnt bones. On either side of the hearth (N

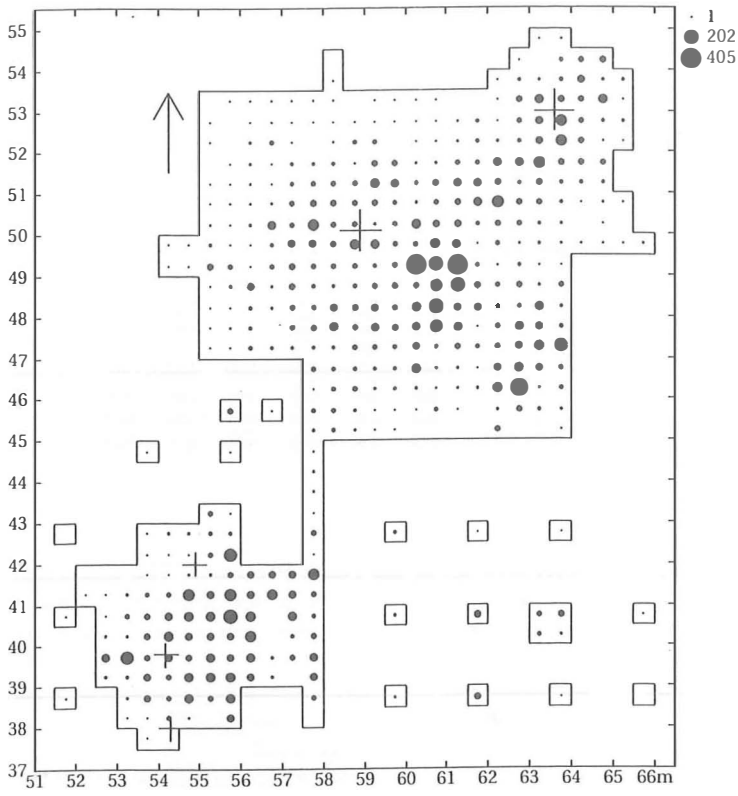

Fig. 25. IT. All artefacts in 1/4 sq.m. cells. N = 15,980. The density map has no classes: every frequency has its own diameter. The diameters of the circles are drawn according to the 'peripheral option', emphasizing the lower frequencies (see Cziesla, 1990; Boekschoten & Stapert, in press). Crosses: hearths.

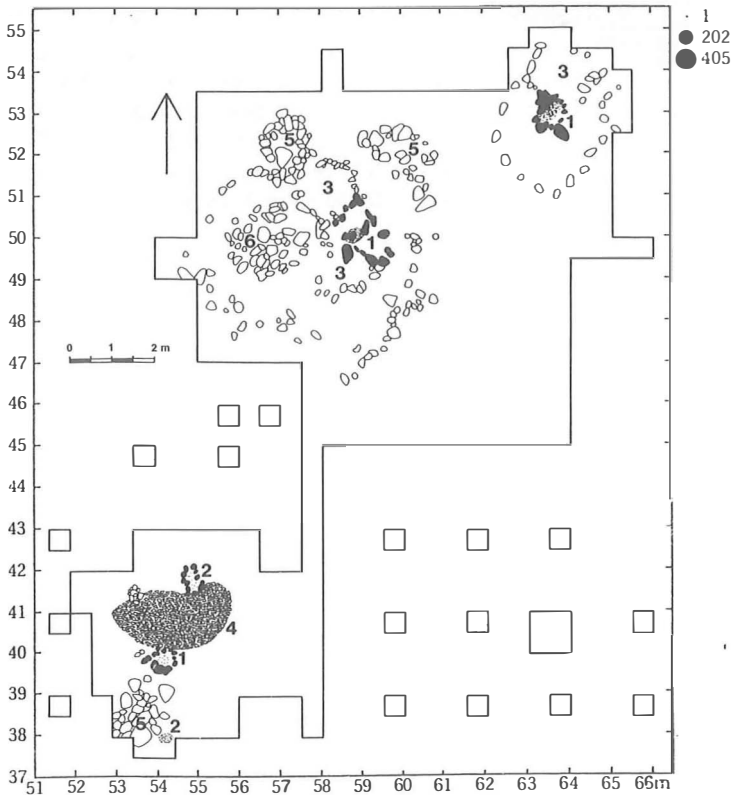

Fig. 26. IT, site-map of the 1993 excavation, in which the main features are indicated. Key: 1. Hearths inside dwelling structures; 2. Peripheral hearths; 3. 'Beds'; 4. Stone platform; 5. Meat caches; 6. Box-like structure. Stones interpreted as structural elements of hearths are indicated in black. Drawing Lykke Johansen.

Table 1. IT, 1993 excavation. Lithic artefacts: quartz, rock crystal, chalcedony and killiaq (silicified slate).

Types	Number	Percentage of subtotal
Tools		
End-scraper	66	11.2
'Side-scraper' (concave)	8	1.4
Bifacial point or knife	87	14.7
Bifacial leaf-shaped tool	28	4.7
Fragment of bifacial tool	37	6.3
Preform of bifacial tool	64	10.8
Burin-like tool	38	6.4
Polished point	11	1.9
Retouched blade or flake	7	1.2
Axe	6	1.0
Polished chisel	2	0.3
Microblade with basal retouch	228	38.6
Saqqaq tool	5	0.8
Other	3	0.5
Subtotal	590	99.8
Percentage of total		3.72
		Percentage of total
Non-tools		
Microblade-core	27	0.17
Flake-core	9	0.06
Nodule	4	0.03
Complete microblade or proximal fragment	334	2.11
Medial or distal fragment of microblade	323	2.04
Blade	5	0.03
Flake	1657	10.44
Chip (<1 cm)	12916	81.41
Subtotal	15275	96.28
Total	15865	100.00

Table 2. IT, 1993 excavation. Artefacts of soapstone.

Types	Number	Percentage of total
Fragment of soapstone lamp	18	41.9
Fragment of soapstone bowl	11	25.6
Bead of soapstone	3	7.0
Facet-cut soapstone	1	2.3
Reworked fragment of soapstone	10	23.3
Total	43	100.1

and S), raised sleeping platforms were observed, consisting of a close-set pavement of small stones with an outer ring of larger stones. In the western part of the house, a box structure made of big slabs was present. In the northern wall of the house there was a meat-cache.

As far as lithic material is concerned, four major groups of raw materials can be discerned. The most important material is the exogenous chalcedony, which comprises many subtypes (between 15 and 25). Some of these subtypes occur clustered within small areas of the site. Furthermore, there are quartz (two subtypes) and rock crystal (two subtypes), both exogenous as well. These are all quite hard materials. Relatively soft materials were also used at IT. A large number of the lithic tools are made of 'killiaq' (three subtypes), a kind of silicified slate. Killiaq is a 'granular' material, unlike both chalcedony and rock crystal. Finally, bowls, lamps and pendants were made of soapstone. None of the

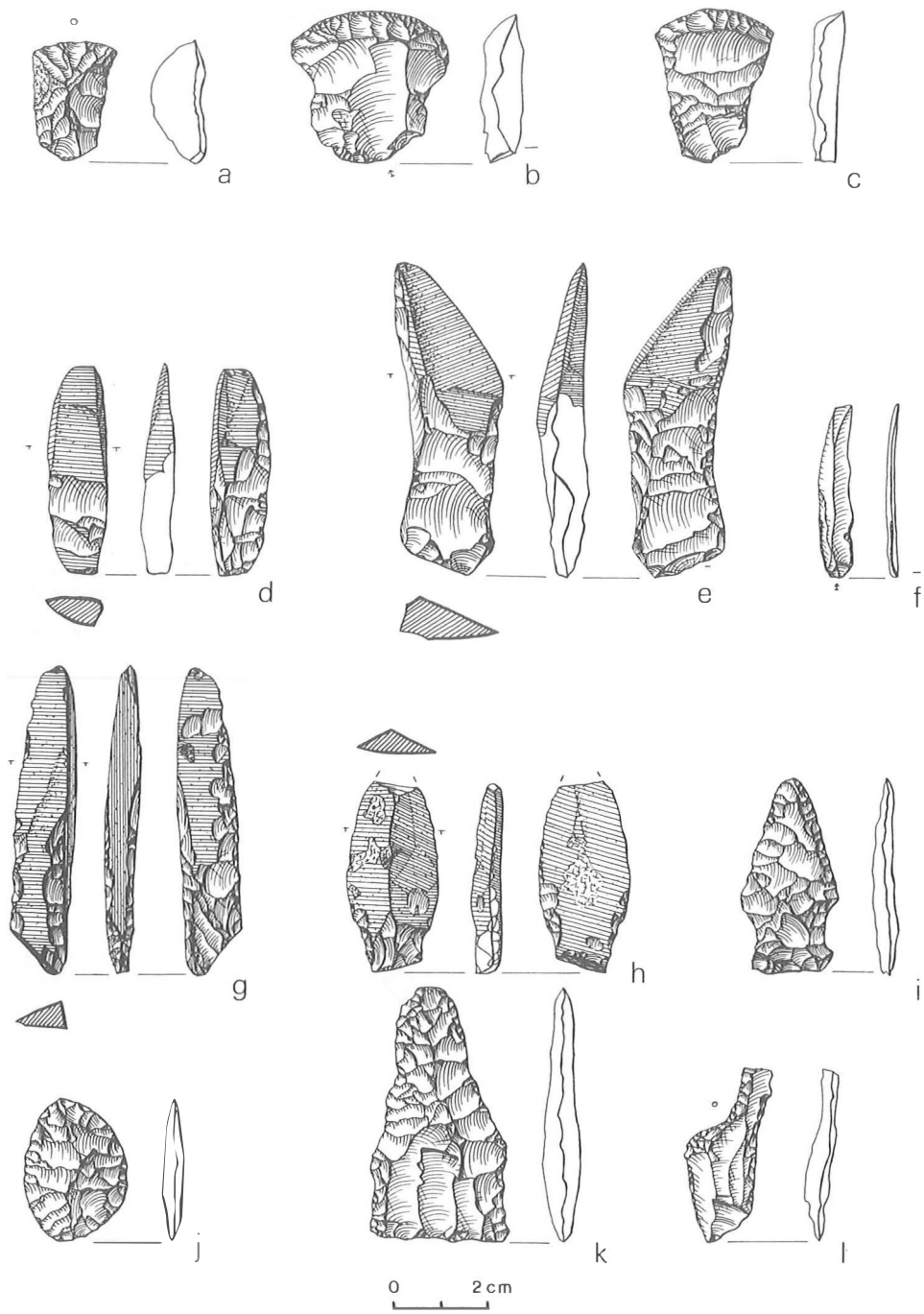

Fig. 27. IT, selection of the tools. a-c. Scrapers; d, e, g. 'Burin-like tools'; f. Microblade with basal retouch; h, i, k. Bifacial points and knives; j. Leaf-shaped bifacial tool ('side-blade'); l. 'Side-scraper'. Drawing Lykke Johansen.

mentioned raw materials is available locally, as far as we know. They were probably all imported over distances larger than 75 km, possibly from the northern coastal zone along Disko Bay or from Disko Island. An overview of the lithic material excavated at IT is presented in tables 1 and 2. In total, 590 tools of non-soapstone materials were collected (fig. 27). These include end-scrapers (a-c), 'burin-like tools' (polished; d, e and g), microblades with basal retouch (f), bifacial points and knives (h, i and k), leaf-shaped bifacial tools ('side-blades'; j) and 'side-scrapers' (concave; l). The numerous microblades are made of chalcedony or rock crystal. Burin-like tools are made of killiaq. The bifacial tools are normally manufactured from chalcedony, but

some are made of killiaq. Tools made of killiaq are mostly polished. A single harpoon head, made of bone, is of early Dorset type.

In this paper, we will concentrate on the dwelling structure in the northern part of the excavation. We analysed the area within 4 m from the centre of the hearth present in its interior. This text is not in the first place meant as a report on the IT site. The IT site appears in this paper especially for the development of methodological ideas concerning the ring and sector approach.

7. GRID-CELL DATA AND SPURIOUS PEAKS

Within 4 m from the hearth inside the analysed dwelling structure, a total of 7317 artefacts were recovered. Only 292 of these (4%) were measured in individually: the tools recognized during excavation. The remainder were collected per quarter square metre by careful sorting through the soil. This tedious procedure is analogous to sieving, and we use the word 'sieving' for this procedure in the remainder of this text. All the chips, pieces smaller than 1 cm, come from the sieve. In the analysed area they number 5829, which is about 80% of the total number of artefacts. An important artefact group are the microblades, some of which have basal retouch. Of their total of 382 within the analysed area, only 46 (12%) have exact coordinates.

Sieved material confronts us with several problems when we want to apply the ring and sector method. In the first place, the cells should not be too large. If sieving is done per sq.m., ring and sector analysis is utterly useless, because such cells are too large. If the soil is sieved per 1/4 sq.m., however, we consider it possible and worthwhile to use the method. The sieved artefacts of IT were given artificial coordinates at the centres of the grid cells. With cells of 50x50 cm, this results in a maximum error of 35 cm. The mean error, however, is only 19 cm, with a standard deviation of 8. Therefore, ring analysis seems justified, if not too narrow rings are employed. It has to be realized, however, that two artefacts originally lying close together might still be estimated to be 70 cm apart.

In the case of IT we used ten rings of 40 cm for most artefact groups. It soon became evident to us that we had to confront problems resulting from the fact that most of the artefacts at IT had been collected per quarter square metre, and given artificial coordinates in the middle of the cells. We repeatedly encountered ring diagrams like figure 28. In this figure, the ring distribution of the chips in sector 7 (of 8; see fig. 46) is shown. It can clearly be seen that there are cyclical peaks, at about every 80 cm. These are caused by the clustering of the chips in the centres of the 1/4 sq.m. cells. With the specific location of the hearth centre used in this case, these 'pseudo-peaks' are especially evident in some sectors to the NW and SE, and less in other sectors. With a different hearth centre, such spurious peaks would have been created in other sectors.

This problem turns up only when distance data are analysed in sectors. If the data from the whole area under analysis are used, as was done in the case of Gönnersdorf III (Stapert & Terberger, 1989), the spurious peaks will not show up, because they are smoothed away. The problem becomes serious especially when four or eight sectors are used, as will be shown in the next chapter.

8. THE USE OF AN ARTIFICIAL DATA FILE

We have to find a way to deal with the distortion created by the sieved artefacts. This is all the more necessary because the excavation technique used at IT is the standard technique nowadays. The degree and the pattern

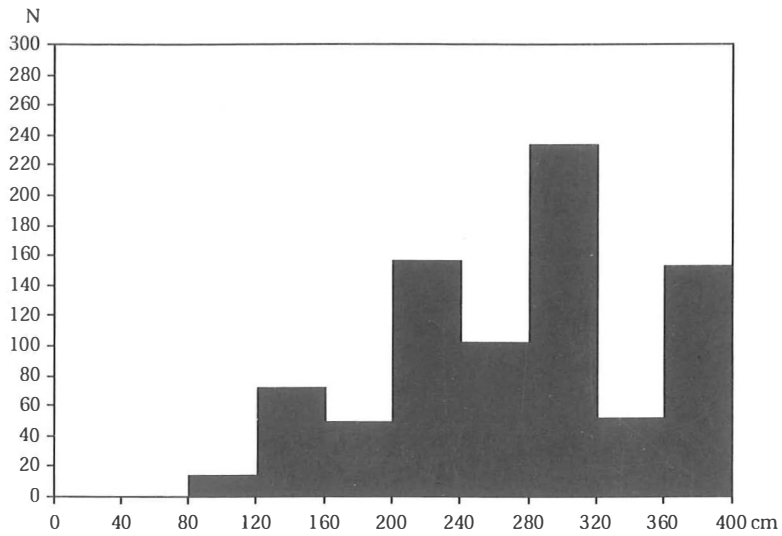

Fig. 28. IT. Ring distribution of the chips (artefacts smaller than 1 cm) in sector 7 (SSE; for sector boundaries see fig. 46). Ten rings of 40 cm are used; zero on the X-axis is the centre of the indoor hearth. Note the cyclical peaks. N = 835.

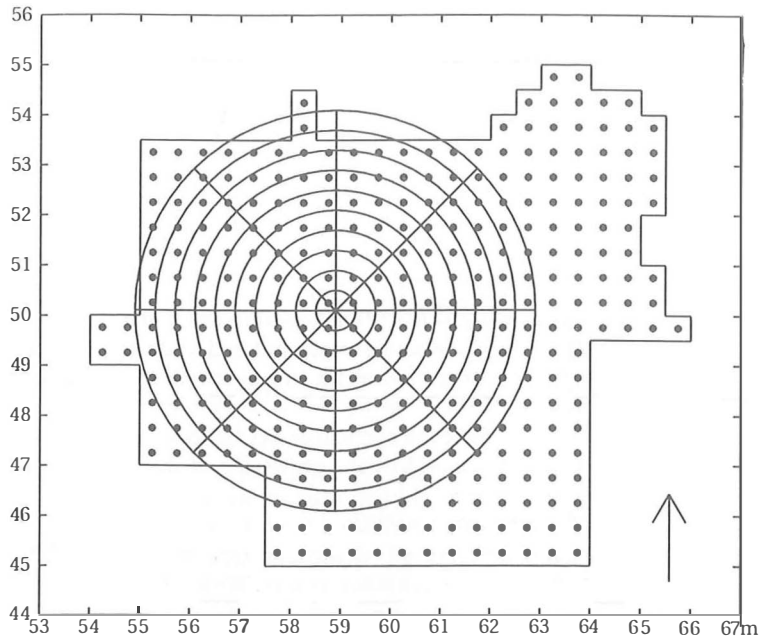

Fig. 29. IT, northern part of the 1993 excavation. The test file, used for comparison with the observed ring distributions. At the centre of each excavated cell of 50x50 cm, one artefact is located. Ten rings of 40 cm and eight sectors are indicated.

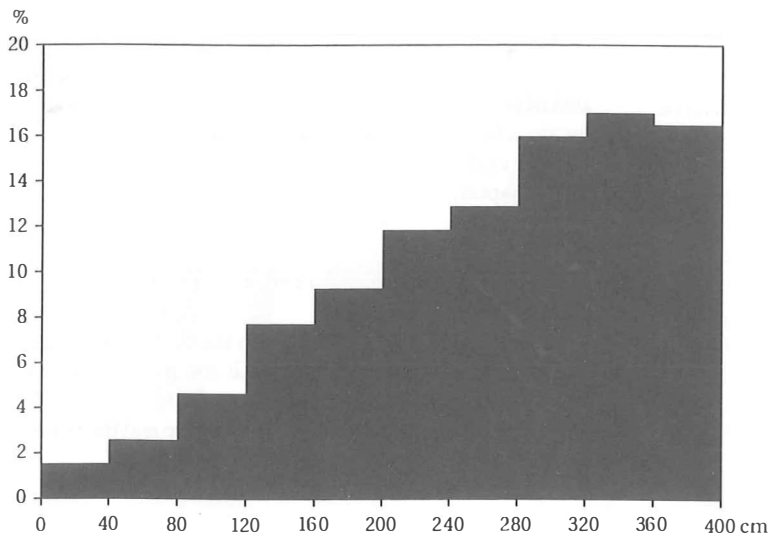

Fig. 30. IT. Ring distribution for the test file (of fig. 29), using 10 rings of 40 cm around the centre of the hearth inside the dwelling at IT: the whole area within 4 m from the centre. Compare with fig. 20. N = 194.

of the distortion can be made visible by using theoretical ring distributions. An artificial test file is created, in which every excavated quarter square metre has one artefact at its centre. The test file for the site of IT is shown in figure 29. Now, with the given 'centre' of the ring analysis, theoretical ring distributions can be created for any selected sector, using any selected ring width. These theoretical distributions, and the observed ones, can be made to show percentages on the Y-axis, instead of frequencies. The R&S program can print out the percentage values in a table.

We can now compare observed ring distributions with the theoretical ones. The ring percentages as found in the theoretical distributions are subtracted from the observed percentages. This produces a curve showing the deviations of the observed distribution from a totally regular spatial distribution, in which the distorting effect of using grid-cell data has been taken into account. This procedure is basically comparable to what we did under 5, but now adapted to the analysis of artefacts deriving from the sieve. Note that in this way also missing ring parts are taken into account. For example, the outermost ring of 40 cm is incomplete at IT, and this will be taken care of by the theoretical distribution.

In figure 30, the theoretical ring histogram is given for the whole area within 4 m from the hearth centre. Note that this graph is almost identical to the one shown

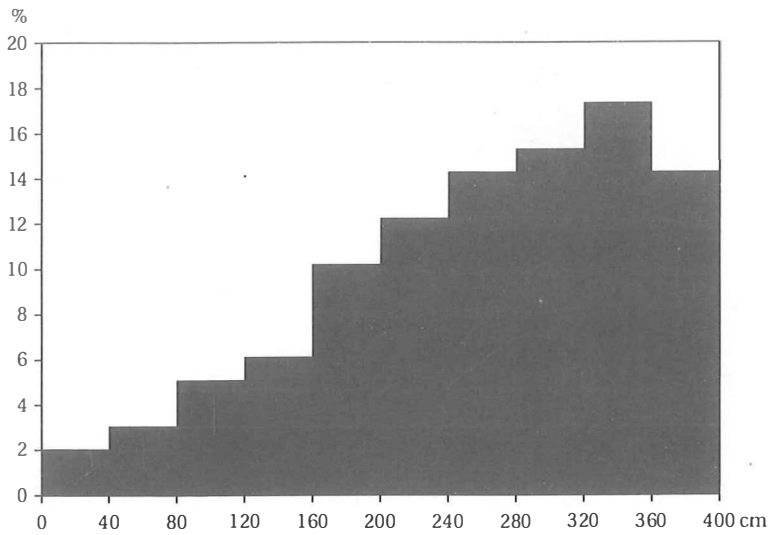

Fig. 31. IT. Ring distribution for the test file: northern half. N = 98.

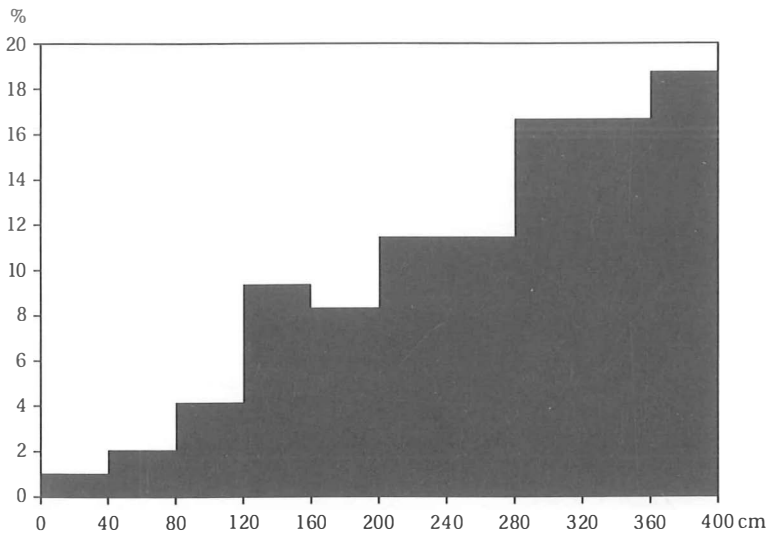

Fig. 32. IT. Ring distribution for the test file: southern half. N = 96.

in figure 20. There are no pseudo-peaks. The incomplete outermost ring has a lower percentage than the penultimate one. We may conclude that if we were to analyse the whole area by the conventional procedure (using raw ring frequencies), significant distortions would not arise. In the analysis of site-halves, the problems begin to be visible. Figures 31 and 32 show the theoretical distributions for the northern and southern halves, respectively. In the diagram for the southern half a small pseudo-peak is visible between 1.2 and 1.6 m. Pseudo-peaks also appear in the theoretical diagrams for the NW and the SE quarters. In the SE quarter especially we can observe the 'cyclical' peaks referred to above (fig. 33). Figure 34 presents the observed ring distribution for the chips in the SE quarter. It is clearly bimodal, with a second peak in the 2.4-2.8 m ring. Now we will see what happens when we subtract the theoretical distribution of figure 33 from the observed distribution: figure 35. The bimodal character is not affected by the distorting effect of the sieving. We still see a first peak in the fourth ring (1.2-1.6 m), reflecting the drop zone near the hearth, and a conspicuous second peak in the seventh ring (2.4-2.8 m), created by the barrier effect of the wall. We may reconstruct the wall of the dwelling, in this quarter, at a distance of about 2.8 m from the hearth centre.

The use of theoretical ring distributions, derived from an artificial test file, has three advantages. In the first place, and most importantly, it makes it possible to use grid-cell data for ring analysis, because it removes the 'pseudo-peaks' resulting from the clustering in the centres of the cells. In the second place, it presents us with the possibility of comparing the observed ring distributions with distributions reflecting randomness. In other words, if peaks are still clearly visible after subtracting the theoretical distribution from the observed

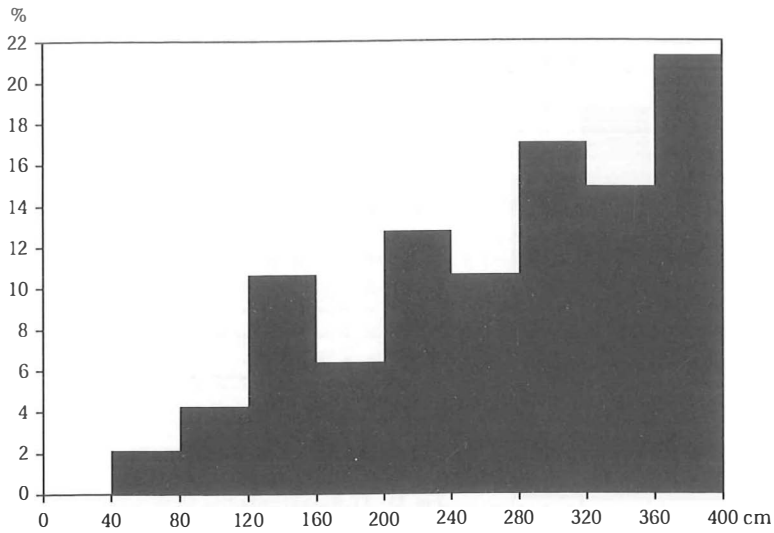

Fig. 33. IT. Ring distribution for the test file: SE quarter. Note the cyclical 'pseudo-peaks'. The Y-axis indicates percentages. N = 47.

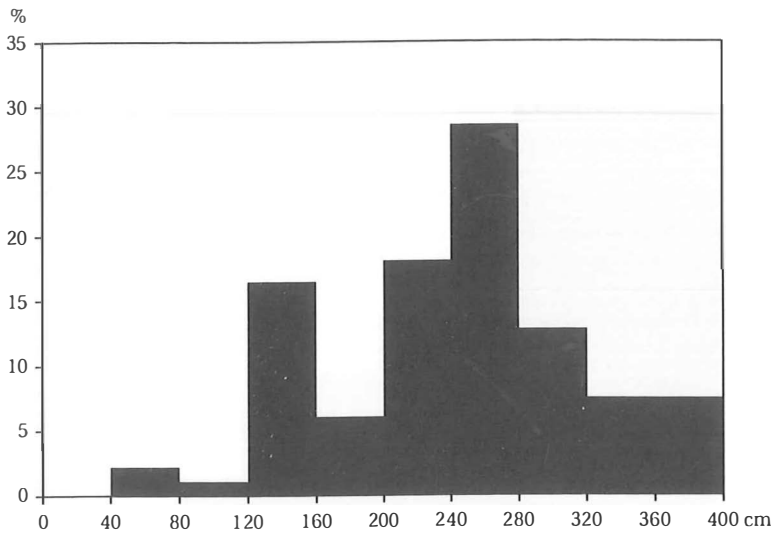

Fig. 34. IT. Ring distribution of the chips in the SE quarter. The Y-axis indicates percentages. Compare with fig. 33. N = 2801.

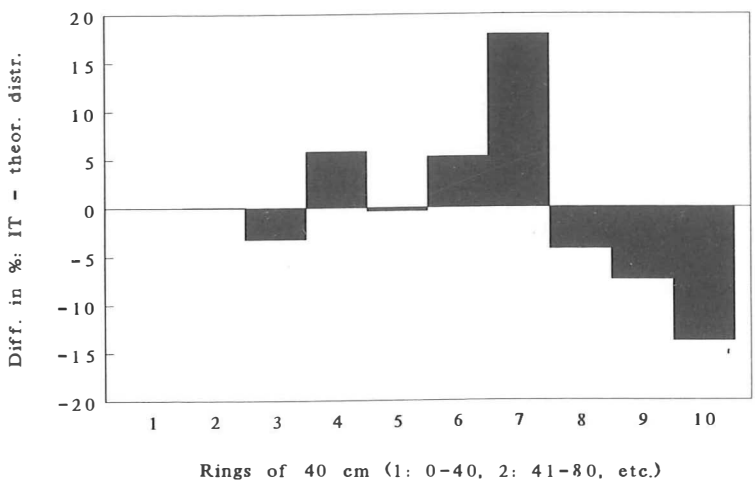

Fig. 35. IT. The ring distribution of chips in the SE quarter, after subtracting the ring distribution of the test file (in both cases the values are expressed as percentages). Note that a conspicuous peak remains in ring 7: 2.4-2.8 m. Compare with figs 33 and 34.

one, we may have greater confidence that we are dealing with real patterns. The third advantage is that the ring distributions are adjusted for missing ring-parts.

9. RECONSTRUCTING THE OUTLINE OF THE DWELLING

In order to make a reliable reconstruction of the outline of the dwelling at IT, we would like to work with at least 8 sectors. The reason is that ring analysis of the area as a whole could result in misleading reconstructions if the hearth was located eccentrically, or if the outline was not round but oval. Performing a ring analysis for eight sectors means that the artefact class subjected to analysis must be quite numerous. If numbers are too small, ring diagrams lose their reliability. For example, it is not possible to study the ring distributions in eight sectors of the bifacial implements. Most of these tools were measured in individually, so it would be desirable to study their ring distributions. However, there are too few of them for this approach. Bifacial tools of all types taken together, including preforms and fragments, total only 91 within 4 m from the hearth centre. Therefore we can only perform a ring analysis of the bifacial implements for the whole area. In figure 36, their ring distribution is presented in the conventional way: frequencies per ring. A conspicuous second peak is present between 2.4 and 2.8 m, suggesting the presence of a dwelling with a diameter of about 5.5 m. Though only 29 (32%) of these implements come from the sieve, it was nevertheless decided to subtract the theoretical distribution given in figure 30 from the observed one. The reason is that this procedure also makes up for missing ring parts. The resulting diagram is presented in figure 37. We see a broad 'drop zone', up to about 2 m from the hearth centre. We then see a much narrower positive peak between 2.4 and 2.8 m, which can be interpreted as resulting from the barrier effect of the wall. Beyond 2.8 m, the curve plummets through the

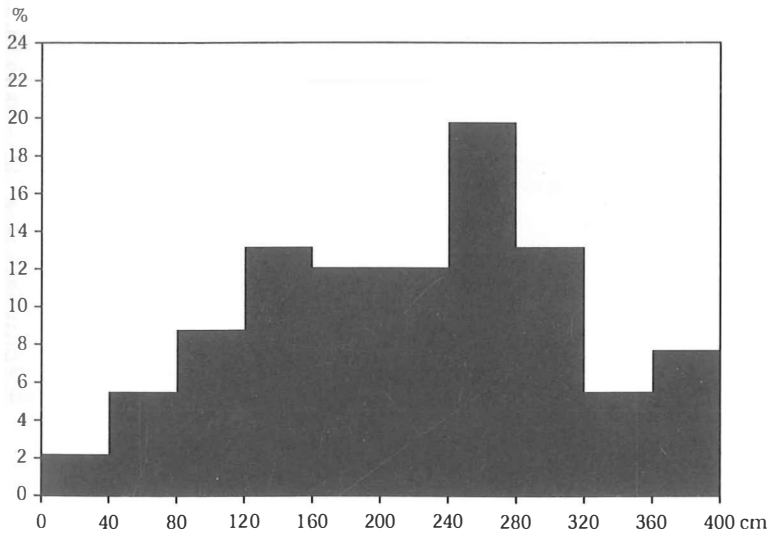

Fig. 36. IT. The ring distribution, over the whole analysed area, of all bifacial tools, including preforms. The values are expressed as percentages. Note the peak in the ring of 2.4-2.8 m. N = 91.

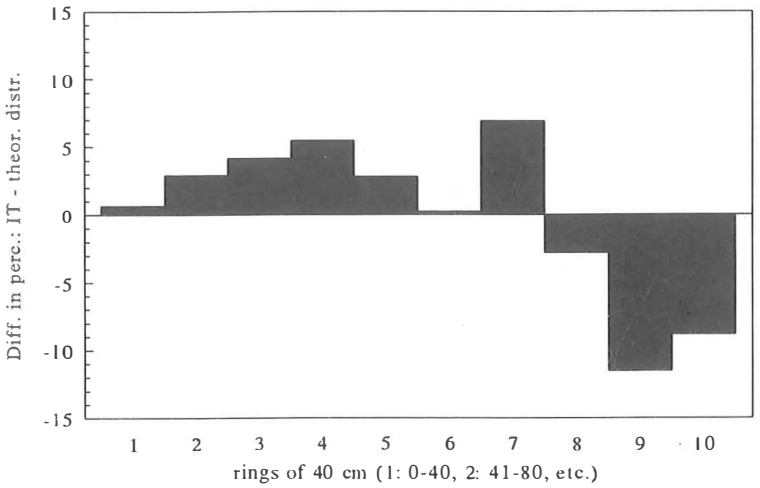

Fig. 37. IT. The ring distribution of all bifacial tools, after subtracting the ring distribution of the test file. Compare with fig. 36.

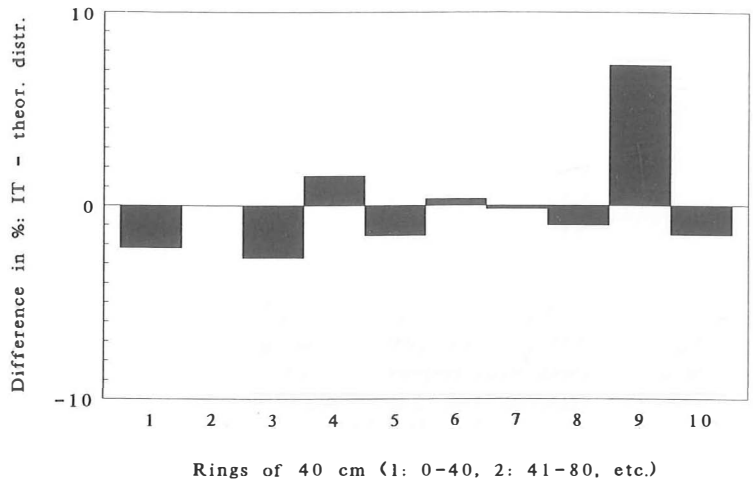

Fig. 38. IT. The ring distribution of the chips in sector 1 (ENE; for sector boundaries see fig. 46), after subtracting the ring distribution of the test file in the same sector. In both cases, the values are expressed as percentages. N = 1015.

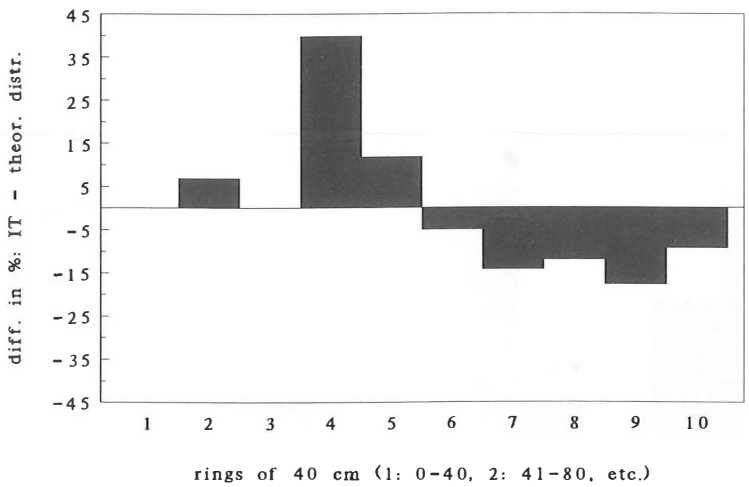

Fig. 39. IT. The ring distribution of the chips in sector 2 (NNE), after subtracting the ring distribution of the test file in the same sector. N = 271.

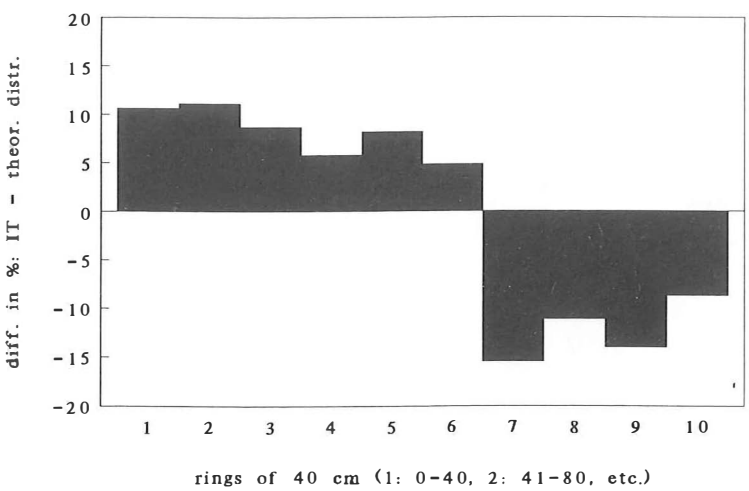

Fig. 40. IT. The ring distribution of the chips in sector 3 (NNW), after subtracting the ring distribution of the test file in the same sector. N = 207.

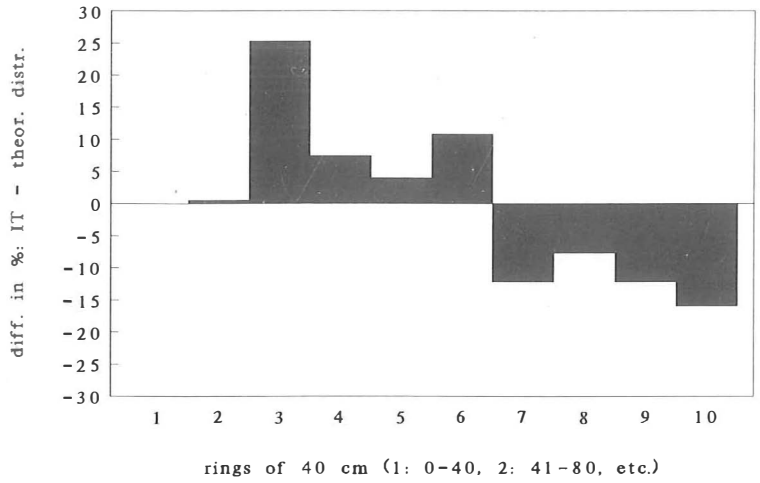

Fig. 41. IT. The ring distribution of the chips in sector 4 (WNW), after subtracting the ring distribution of the test file in the same sector. N = 379.

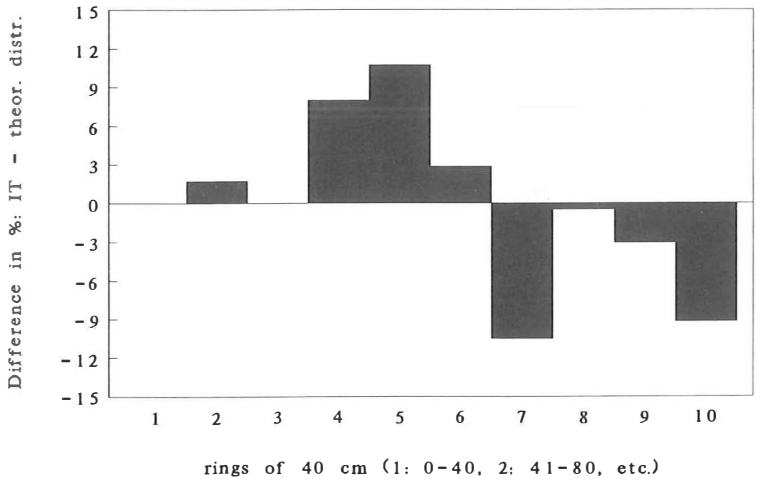

Fig. 42. IT. The ring distribution of the chips in sector 5 (WSW), after subtracting the ring distribution of the test file in the same sector. N = 510.

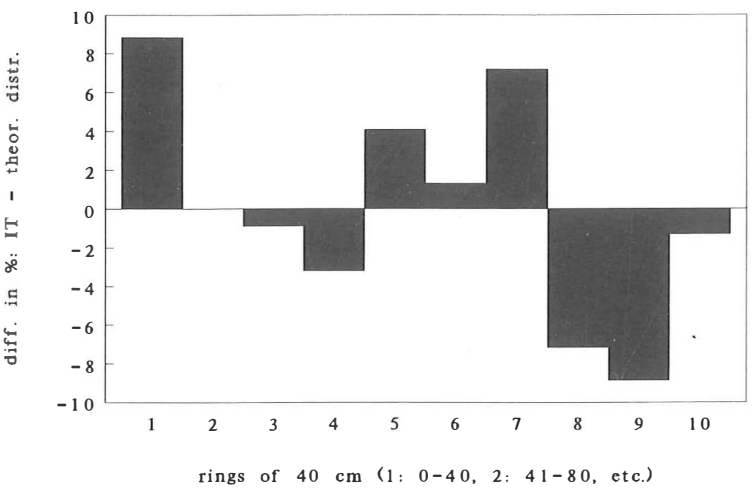

Fig. 43. IT. The ring distribution of the chips in sector 6 (SSW), after subtracting the ring distribution of the test file in the same sector. N = 646.

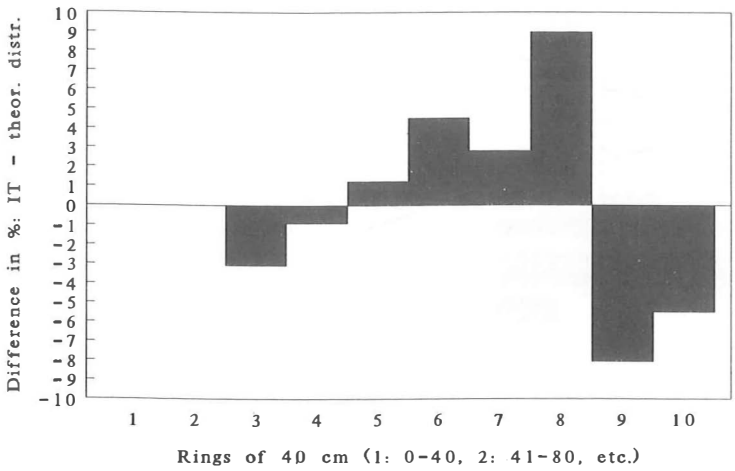

Fig. 44. IT. The ring distribution of the chips in sector 7 (SSE), after subtracting the ring distribution of the test file in the same sector. N = 835.

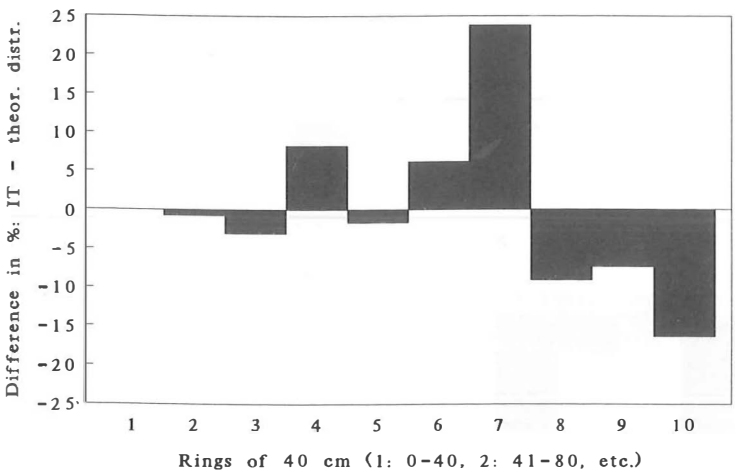

Fig. 45. IT. The ring distribution of the chips in sector 8 (ESE), after subtracting the ring distribution of the test file in the same sector. N = 1966.

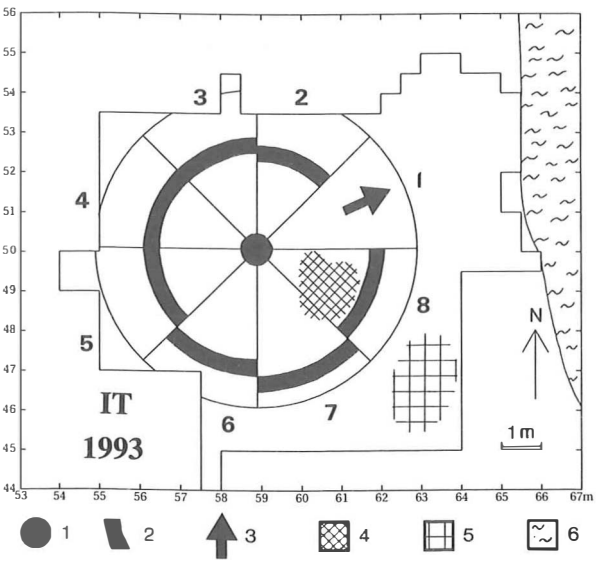

Fig. 46. IT. Reconstruction of the dwelling in the northern part of the 1993 excavation, based on the ring distributions of chips in eight sectors (figs 38-45). Key: 1. Hearth; 2. Reconstructed wall of the dwelling; 3. Supposed entrance; 4. Working area (resharpening etc. of lithics) inside the dwelling; 5. Dump outside the dwelling; 6. Coast line. Drawing Lykke Johansen/Dick Stapert.

zero line. Figure 37 supports the hypothesis that there was indeed a dwelling here. It does not, however, allow us to reconstruct its outline with any precision.

As noted earlier, chips constitute the most numerous artefact group at IT. Within 4 m from the hearth centre, there are 5829 chips (79.7% of all artefacts). Their number is sufficiently high to allow the study of ring distributions in eight sectors. Thanks to the use of theoretical distributions, it is now possible to use these artefacts, which all come from the sieve. It has been argued that especially tool locations are suitable for ring and sector analysis, if one wishes to investigate the presence/absence of walls (Stapert, 1989: pp. 4-5). Chips would be expected especially to occur clustered at knapping locations. In the case of IT, however, the chips are thought to derive from repairing or resharpening of imported tools (see 6 and 12).

Figures 38-45 present the ring distributions of the chips in eight sectors, compared to the theoretical distributions for the same sectors. In most sectors, the 'wall effect' can clearly be seen. However, the points where the curves cross the zero line after the second peak are not everywhere at the same distance from the

hearth. This suggests that the hearth was located not exactly in the middle of the dwelling, which moreover probably had a somewhat oval outline. In our reconstruction of the house, based on the analysis of the chips, it has an inner diameter of 5-5.5 m (fig. 46). A more or less identical outline is found when all artefacts with individual coordinates (mostly tools) are analysed, though their number is relatively low.

10. RING PAIRS

Both drop zones and zones of accumulation against the walls of dwellings due to the barrier effect, will produce peaks in ring distributions. Theoretically, it is not imperative that these peaks should be positive in the curves we used in the last chapter. If they are indeed positive, they stand out quite clearly in the curves, so we can feel confident that we are dealing with real patterns. There is another way, however, to look at these diagrams, which is closer to the nature of the phenomena we are dealing with. Drop zones and accumulation zones against walls of dwellings in fact imply that ring frequencies first increase and then decrease, going outwards from the hearth. With the second peak, reflecting the barrier effect of the wall, in many cases the decrease especially should be quite dramatic, because few if any artefacts would have ended up within the wall. (However, this effect could be dampened to some degree through the chosen ring width. If the wall starts in the middle of a ring, part of the abruptness will be lost. The same is true when the hearth is not exactly in the middle of the dwelling.)

This sequence of increase and decrease should always show up, whatever kind of transformation of the raw frequencies is employed. It is therefore of interest to compare pairs of consecutive rings with each other: first rings 1 and 2, then rings 2 and 3, etc. For 10 rings, we then get 9 values, positive or negative, showing in each case whether the next ring frequency is higher or

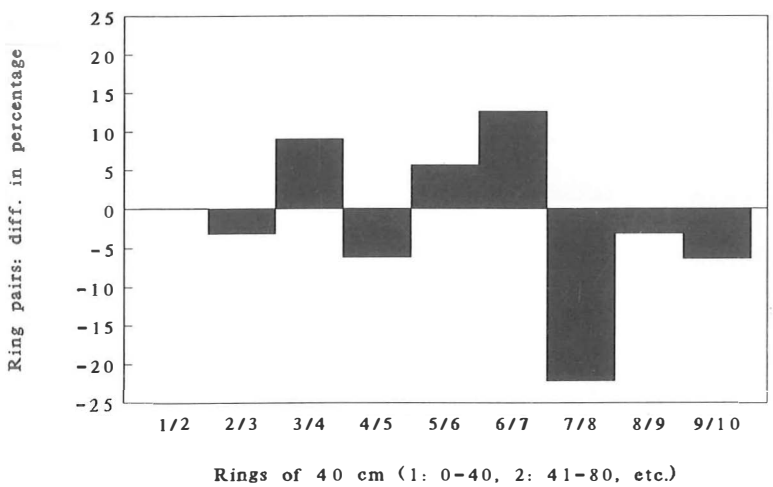

Fig. 47. IT. Chips in the SE quarter. Differences (in percentage) between pairs of consecutive rings, after subtracting the theoretical ring distribution, for the SE quarter (compare with fig. 35). Note the dramatic 'fall off' going from ring 7 to ring 8, indicating the position of the wall. N = 2801.

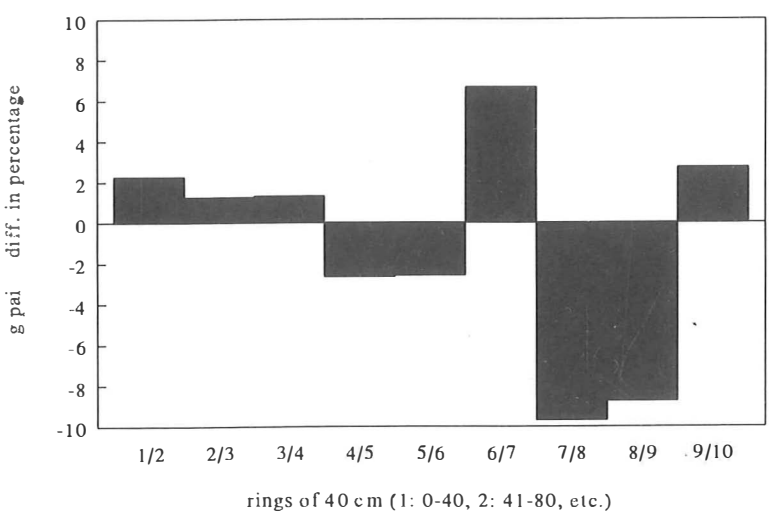

Fig. 48. IT. All bifacial tools, including preforms, in the whole analysed area; rings of 40 cm. Differences (in percentage) between pairs of consecutive rings, after subtracting the theoretical ring distribution (compare with fig. 37). Again we see a conspicuous 'fall off' going from ring 7 to ring 8. N = 91.

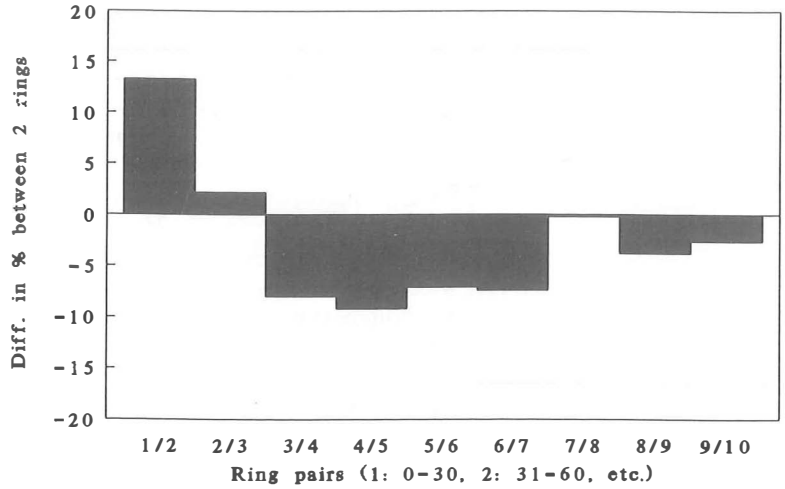

Fig. 49. Pincevent T112. Tools in rings of 30 cm. Differences (in percentage) between pairs of consecutive rings, after subtracting the theoretical ring distribution (compare with fig. 22). As at Oldeholtwolde (fig. 50), the curve does not return to the positive area after having dipped below the zero line. N = 334.

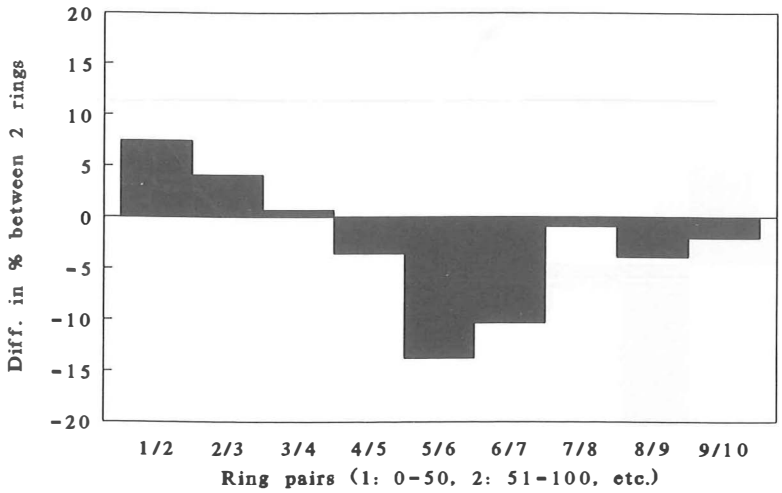

Fig. 50. Oldeholtwolde. Tools in rings of 50 cm. Differences (in percentage) between pairs of consecutive rings, after subtracting the theoretical ring distribution (compare with fig. 23). N = 264.

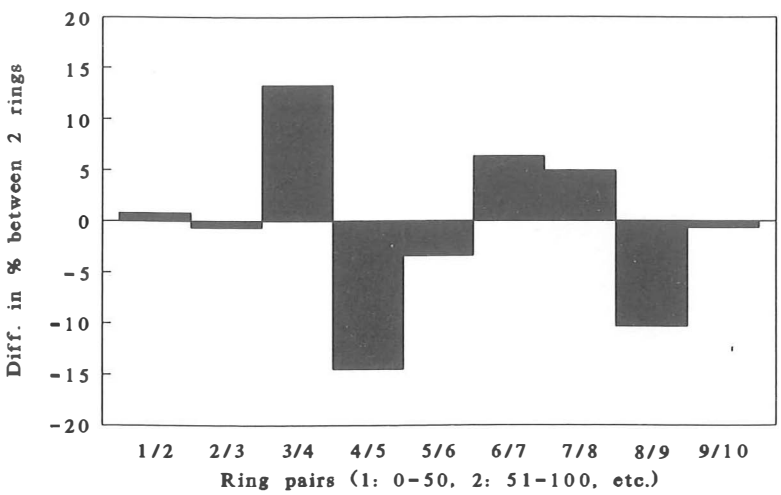

Fig. 51. Gönnersdorf II. Backed bladelets in the NW quarter; rings of 50 cm. Differences between pairs of consecutive rings, after subtracting the theoretical ring distribution (compare with fig. 24). As at IT, the presence of a wall can be observed. N = 72.

lower than the preceding ring frequency. Of course, when analysing chips at the IT site, we should use the values found by subtracting the theoretical ring percentages from the observed ones. To illustrate this kind of curve, the chips in the SE quarter of IT will be used. Using the ring percentages found by subtracting the theoretical distribution from the observed one (see fig. 35), we get the curve shown in figure 47. There is an increase going from ring 6 to ring 7, and a sharp decrease going from ring 7 to ring 8. This is the kind of pattern that we should expect to see when a wall is present. Figure 48 presents the curve showing differences between ring pairs for the bifacial implements, including preforms (compare with figs 36 and 37). Again the 'wall effect' is very obvious. Going from ring 7 to ring 8, there is a sharp decrease – indicating the position of the wall.

As further illustrations of this 'ring-pair curve', we present the distributions (compared to the theoretical distributions) of Pincevent (fig. 49; compare with fig. 22), Oldeholtwolde (fig. 50; compare with fig. 23) and Gönnersdorf II: backed bladelets in the NW quarter (fig. 51; compare with fig. 24). The point of these curves seems to be the following. In the case of open-air hearths, the curve does not return to the positive area after having dipped below the zero line; in the case of hearths inside dwellings it does – just inside the wall – after which it plummets quite dramatically. This kind of curve, showing increase or decrease in pairs of consecutive rings, after subtraction of the theoretical distribution, is in our opinion quite useful in demonstrating the absence of presence of walls of any kind. We hope to explore this approach more fully in the coming years, in cooperation with Akili Software in Groningen.

11. LOCATING THE ENTRANCE

At site IT, the richest area in terms of artefact numbers is located about 2 m to the southeast of the hearth (4 in fig. 46). This is an area where lithic materials were worked, though it could partly be a dump; chips and flakes especially are very numerous here. It has a diameter of about 1.5 m. Quite a number of different types of raw material have been worked here, in many episodes: at least ten subtypes of chalcedony, cream-coloured killiaq, and cracked rock crystal. Probably transparent rock crystal was worked here too, but that material was worked predominantly in an area of its own: immediately north of the hearth (see also section 13). About 2 m to the southeast of the main working area for lithics, there is another area with high artefact numbers (5 in fig. 46). Our impression, based on refitting, is that this latter area for the most part at least was a dump.

At Gönnersdorf II, there are also indications for a dump outside the dwelling (also to the southeast of it; see Boekschoten & Stapert, 1993: fig. 10). Inside the tent, the southeastern quarter is also the richest in tool numbers. Therefore, it seemed obvious that the richest sector, of, for example, eight sectors, would indicate the position of the tent entrance, because during occupation there would have been a continuous movement of waste material towards the entrance and the doordump located outside it. However, a door dump could have been located to one of the sides of the entrance, or at some distance, and in such cases the richest-sector approach for locating the entrance might produce misleading results.

Theoretically, the best way of locating the entrance of dwellings is to look for a sector where the barrier effect of the wall cannot be demonstrated. In other words, we may expect the entrance to be located in the sector where a second peak in the ring diagram is absent or insignificant. In the case of IT, the ring diagram of the chips in sector 1 (ENE of the hearth) does not show the wall effect (fig. 37). There is only one conspicuous peak, which is in the area between the dwelling and the tent ring. We might be dealing here with a small door dump, shared by the tent and the dwelling, but one or several outdoor activity areas were also located here. At least some resharpening of tools (axes, burin-like tools) was done. For example, this area yielded quite a lot of dark-grey killiaq chips and flakes with polishing. The most probable location of the entrance of the dwelling seems to be the ENE (see fig. 46).

It has proved useful to make maps showing all cells containing at least 10, 15, 20, etc., chips. At a certain level the outline of the dwelling should become visible in this way. In figure 52, all cells of 50x50 cm containing at least 30 chips are illustrated. The dense scatter of artefacts in the southeast, supposedly a dump, is not connected to the interior of the house; there is an empty zone about 0.5 m wide between the dump and the working area for lithics. It seems, therefore, that the wall was located between this working area, inside the dwelling, and the dump outside it, as was already indicated by the ring diagrams of the chips shown above. In the northeast, on the other hand, there is a zone of cells rich in chips emerging from the dwelling and joining up with the concentration of artefacts inside the tent ring. Therefore, the entrance could have been located in the NE.

In figure 53, all cells containing at least 4 artefacts that are not chips or flakes are indicated. For the northeast and the southeast, the picture we found for the chips is repeated. Figure 53 again suggests a location of the entrance in the northeast. A difference from the distribution of the chips (fig. 52), however, is that now additional concentrations to the northwest and the south can be observed, outside the dwelling. Here, specialized outdoor activity areas may have been present. The northwestern concentration is connected with two raw materials represented hardly anywhere else on the site: olive-green chalcedony with pale yellow and black

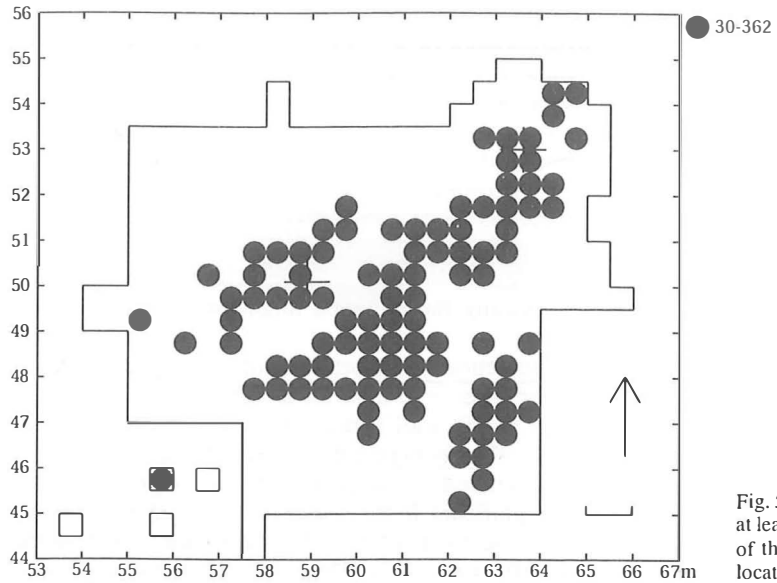

Fig. 52. IT. Map showing all cells of 50x50 cm containing at least 30 chips. Note the empty zone between the interior of the dwelling and the dump to the southeast of it: the location of the wall?

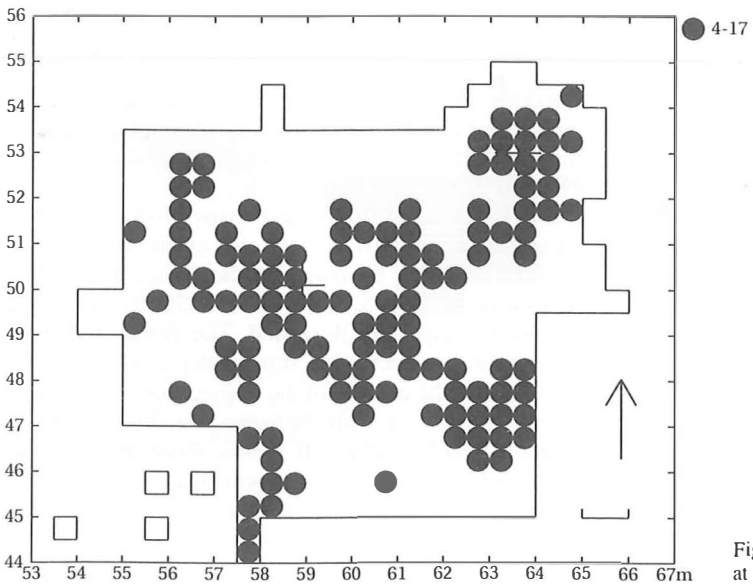

Fig. 53. IT. Map showing all cells of 50x50 cm containing at least 4 artefacts that are neither chips nor flakes.

stripes, and white chalcedony with red/brown spots. The artefacts made of these materials comprise 18 microblades, some with basal retouch, and about ten chips, occurring tightly clustered. This area also produced some bifacial tools, including a few preforms, of other materials. Furthermore, there is a concentration of burnt material in this area. There is no way to tell whether or not this activity area is contemporaneous with the occupation of the dwelling. The concentration to the south is an area where dark-grey killiaq was worked (see also sections 12 and 13). Large numbers of chips and flakes of this material occur both inside and outside the reconstructed wall of the dwelling.

12. REFITTING ANALYSIS

Among the artefacts of quartz, rock crystal, chalcedony and killiaq, a total of 384 could be refitted. This is 13.0% of all artefacts larger than 1 cm of these materials (n = 2949). The refitting percentage is rather low, which reflects the fact that only very few, if any at all, of the tools found at the site were produced there. Chips, pieces smaller than 1 cm, are the dominating artefact class at IT. They were not included in the refitting analysis. Most of the chips probably do not result from primary knapping, but from resharpening of tools and reworking of broken tools. On the tools, especially on the burin-like tools and the axes, but also on the scrapers,

Table 3. IT, 1993 excavation. Refitting analysis of artefacts other than chips of quartz, rock crystal, chalcedony and killiaq (silicified slate): refit types. Key: ( ): Number of fire-cracked artefacts; they are included in the total per type; [ ]: Number of artefacts in a sequence that consist of several fragments (refitted); these are counted here as one; *: Refitting groups containing both breaks and sequences are counted only once: under B.

Type	Number of artefacts	Number of ref. groups*
A. Breaks		
Broken tools (except retouched microblades)	36 (2)	18 (1)
Broken retouched microblades	27 (2)	13 (1)
Broken unret. microblades	141 (26)	60 (12)
Broken flakes	59 (6)	23 (3)
Subtotal	263 (36)	114 (17)
B. Dorsal/ventral sequences		
Microblades	31 [14]	10
Flakes	90 [10]	38
Subtotal	121 [24]	48
Total		162

Table 4. IT, 1993 excavation. Refitting analysis of artefacts other than chips of quartz, rock crystal, chalcedony and killiaq (silicified slate): raw materials. Key: A. Number of non-chips; B. Number of refitted broken artefacts; C. Number of refitting groups: breaks (refitting groups containing both breaks and sequences are counted only once: under E); D. Number of ventral/dorsal refitted artefacts (sequences); E. Number of refitting groups: sequences; F. Total number of artefacts involved in refitting groups; G. Refitting percentage.

Raw material groups	A	B	C	D	E	F	G
Killiaq	748	33	12	57	23	90	12.0
Quartz	10	2	1	0	0	2	20.0
Rock crystal	326	16	7	5	2	21	6.4
Chalcedony	1865	212	94	59	23	271	14.5
Total	2949	263	114	121	48	384	13.0

traces of resharpening and reworking can often be observed. Many points from which the tip had broken off were repaired by resharpening around all the edges except for the basal part. A reduction in size happened several times during the functional 'life-span' of many IT tools. Preforms of various tool types were imported to the site, often in quite an advanced phase of production. Many preforms of bifacial tools have been heat-treated in an earlier stage of the production sequence. Only four 'nodules' (unworked pieces of raw material) are present at IT, which all have shapes and dimensions suitable for exploitation as microblade-cores.

The most common type of refit is between parts of broken artefacts: 64.8% of all refitted artefacts (included are breaks resulting from fire). Artefacts refitted ventrally/dorsally come second: 35.2%. For an overview of the results of the refitting analysis, see tables 3 and 4. Significant differences exist between the various types of raw material in terms of refitting percentage. Killiaq and chalcedony have relatively high refitting percentages. The refitting percentage of rock crystal is lower, because this material is much more difficult to refit. The relatively high refitting percentage for quartz is due to the fact that there are so few artefacts of this material.

The number of refitted sequences (ventral/dorsal) is higher for killiaq than for chalcedony, which is interesting because chalcedony artefacts are much more numerous. The reason probably is that killiaq tools were reworked more often after they broke or were damaged through use, because killiaq artefacts are on average larger than chalcedony artefacts. Most, or possibly all, of the refitted production sequences of chalcedony do not document knapping on the site, but series of microblades produced elsewhere.

As noted above, refits of broken artefacts constitute the largest proportion of refits. Most refitted breaks concern microblades: 144 fragments fit together, resulting in 70 microblades, some of which still are incomplete in the refitted state (fig. 54). The relatively large number of refits of broken microblades reflects the fact that microblades are very thin and therefore apt to break. The risk of breakage would have been high especially when microblades were used as 'knives'. Apart from retouched microblades, 36 tool fragments

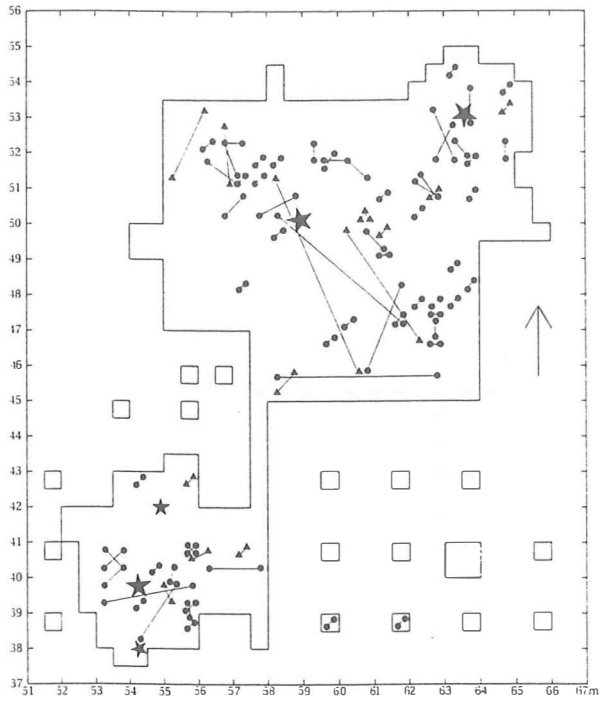

Fig. 54. IT. Map showing refits between fragments of microblades. Key: circles = unretouched microblades; triangles = retouched microblades; large stars = central hearths inside dwellings; small stars = 'satellite hearths'. Drawing Lykke Johansen.

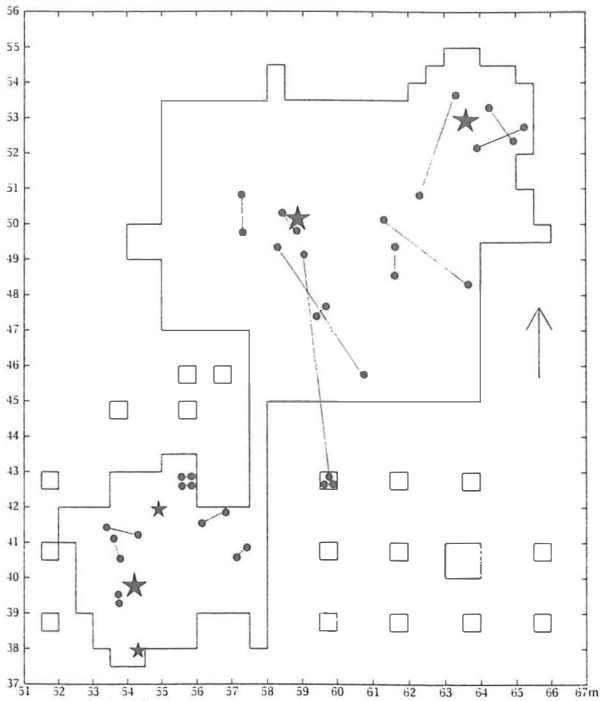

Fig. 55. IT. Map showing refits between fragments of tools other than retouched microblades. Drawing Lykke Johansen.

were refitted to 18 tools of other types (fig. 55); most breaks probably occurred as a result of use.

Two fitting fragments of a microblade with retouch were more than 6 m apart: the distal fragment was found in the northern 'bed' inside the dwelling, while the proximal fragment was outside the dwelling – to the SE of it. Of a second broken retouched microblade also, the distal fragment occurred inside the dwelling, and the proximal fragment to the SE of it. Fragments of two broken retouched microblades lay close together in the entrance area of the dwelling. Two refits of broken tools of types other than retouched microblades also show fairly long connecting lines, in both cases connecting the southern 'bed' inside the dwelling to the outside area SE of it.

Refittable fragments of unretouched microblades occur clustered in the northern part of the dwelling and in the dump area to the SE of it. A refit over a longer distance connects the hearth inside the dwelling with the dump area to the SE. Relatively many refits occur over short distances around the meat cache and just outside the dwelling – to the NE and SE of it. Most refits between flake fragments (fig. 56) occur around the hearth inside the dwelling. One refit connects the interior of the dwelling with an area to the S.

Series of ventrally/dorsally refitted microblades (all unretouched) are rare inside the dwelling (fig. 57). Interesting are two series: one connecting the box

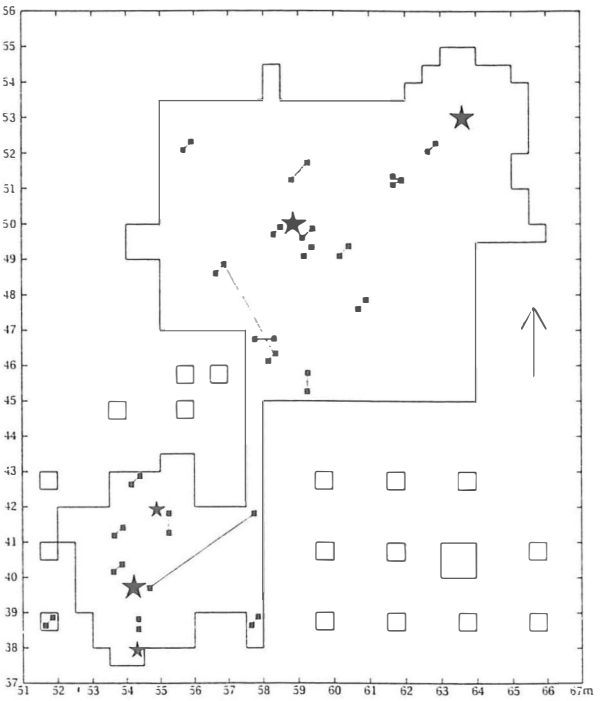

Fig. 56. IT. Map showing refits between flake-fragments. Drawing Lykke Johansen.

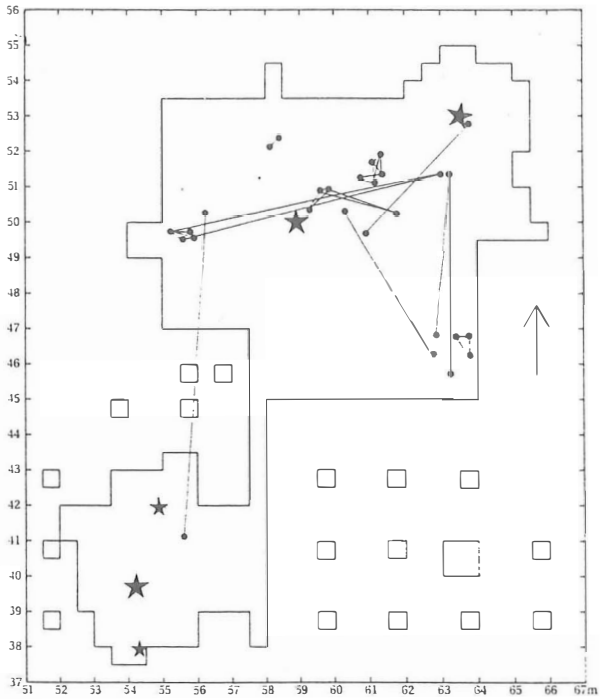

Fig. 57. IT. Map showing ventral/dorsal refits of microblades. In figs 57 and 58, some refits of breaks are indicated too, if they are part of the illustrated sequence; these refits are drawn as -.-. Drawing Lykke Johansen.

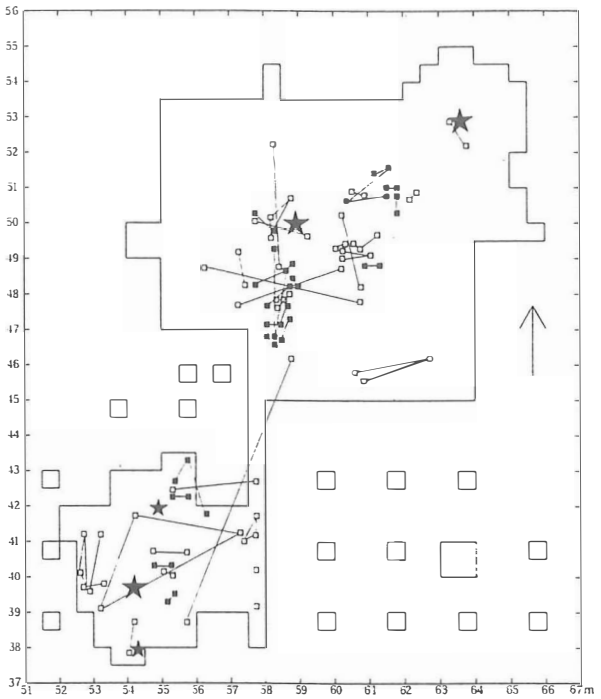

Fig. 58. IT. Map showing ventral/dorsal refits of flakes. Key: black squares = dark-grey killiaq; white squares = flakes of other materials. Drawing Lykke Johansen.

structure inside the dwelling with the 'platform' in the southern part of the excavated area, the other connecting the box structure inside the dwelling with the tent ring to the northeast. Another refit connects the entrance of the dwelling with the dump to the SE of it. There is also a refit between two microblades one of which lay in the entrance area of the dwelling and the other near the hearth in the NE tent ring. Several series of refitted microblades have connecting lines involving the entrance area of the dwelling. One series of three microblades connects the tent ring in the NE with the dump to the SE of the dwelling. The ventral/dorsal series of microblades show remarkably many refits over long distances, connecting the three main dwelling structures. This brings up the question of possible 'scavenging' of lithics from older, abandoned dwellings. This is a realistic option in the case of the IT site, because all raw materials had to be imported. In this connection it may be mentioned that although there are 27 microblade-cores at IT (all of rock crystal), it has not been possible to refit a single microblade to any of these. Rock crystal is a difficult material to refit. Nevertheless, it is probable that most of the ventral/dorsal series of microblades were produced elsewhere, and this is certainly true for the microblades of chalcedony. The majority of microblades are made of chalcedony. All series are very short, comprising no more than two or three microblades.

Dorsal/ventral refits of flakes (fig. 58) are heavily dominated by flakes of dark-grey killiaq. Several series occur around the hearth inside the dwelling. Quite a few ventral/dorsal series of killiaq were found in the entrance zone of the dwelling, or to the south of it. The lines of several series crossing the postulated southern wall of the dwelling are particularly interesting. They might represent activities dating from after the habitation of the house (however, see also section 13). As in the case of ventral/dorsal series of microblades, series of flakes are very brief, comprising two to four flakes only. No primary knapping seems to have been going on. The series of dark-grey killiaq probably all document the repairing of axes, or the reworking of broken or damaged axes into chisels or burin-like tools.

In the case of IT, refitting analysis cannot tell us much about the position of the walls. One of the few indications is the occurrence in the supposed wall zone (especially to the north of the hearth) of short lines between refitted breaks, for example of microblade fragments (fig. 54).

Regarding the stones interpreted as structural elements, the dwelling seems to be more heavily disturbed than the tent ring to the NE. This might indicate a different building style, but it might also mean that the dwelling was erected earlier than the tent, and was scavenged for stones later.

Both to the left and right of the supposed entrance of the dwelling (in the ENE), outside the house, there seem to have been activity areas and/or door dumps, because there are higher numbers of refits there than inside the

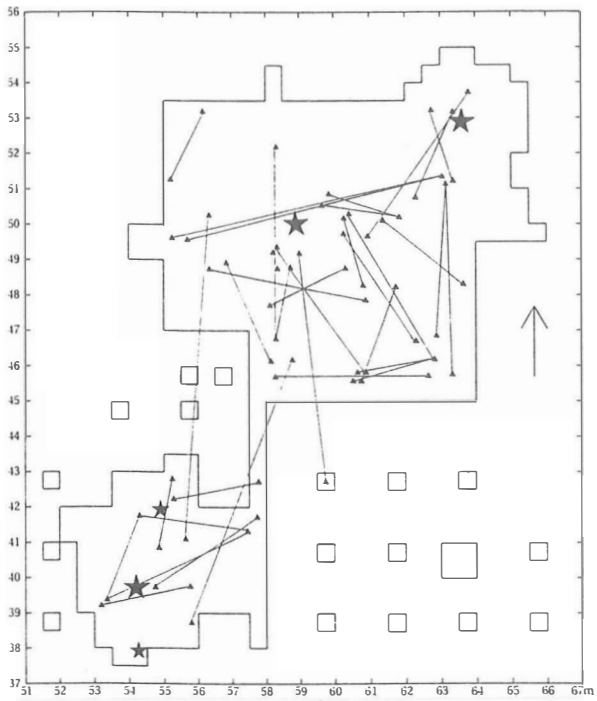

Fig. 59. IT. Map showing all refitting lines longer than 2 m (both breaks and sequences). Drawing Lykke Johansen.

dwelling. In figure 59, all refitting lines longer than 2 m have been mapped. Many refitting lines indicate the presence of a dump area outside the dwelling, to the SE of it. Refitting analysis indicates that this dump was used both by the inhabitants of the dwelling and by those of the tent in the NE. From ethnographic sources about Inuit people we know that when the occupants of a winterhouse break up in the spring, a small group will sometimes stay behind, composed mainly of older people. The stay-behinds then tend to move out of the house into a tent. This might have been the case at IT. Maybe something similar happened in the case of the large structure at Gönnersdorf I and the tent ring located near to it (see Bosinski, 1979; Franken & Veil, 1983).

13. RAW MATERIALS AND SPATIAL PATTERNS

For the area within 4 m from the centre of the hearth inside the dwelling in the northern part of the excavation, artefact numbers of four raw material groups (quartz, chalcedony, rock crystal and killiaq) are given in table 5. In this section we shall investigate whether or not these raw materials show different spatial distributions. For this, we will use both density maps and sector graphs. Quartz artefacts are clustered in the extreme east of the excavated area, and there are hardly any artefacts of this material inside the dwelling, so we shall not further discuss this material here. Chalcedony, rock crystal and killiaq occur in large numbers, also inside the dwelling. Each of these raw materials has several sub-types, showing different distributions in space.

The second author has distinguished 25 sub-types of chalcedony at IT. Of 11 sub-types of chalcedony there are less than 10 artefacts per sub-type within 4 m from the hearth centre; these are not discussed here. Of the remaining 14 sub-types of chalcedony, sector graphs were produced for all chips and flakes together. Sector graphs are in fact a combination of a pie chart and a bar graph (see Boekschoten & Stapert, 1993; in press). The area within 4 m from the hearth centre is divided into 8 sectors (see fig. 46). In a sector graph, the centre of the 'wheel' has the value zero. The circle represents the average number of artefacts per sector. Sectors with a number of artefacts higher than the mean have a black bar protruding outwards, sectors below the mean have a white bar extending inwards. In this way one can easily establish in which sector the raw material in question has its greatest amount of flint waste (chips and flakes). Ten of the fourteen sub-types of chalcedony have their richest sector in the SE: the reworking/repairing location indicated in figure 46: 4. A density map of the chips and flakes of all of these ten sub-types of chalcedony together, is presented in figure 60. It can be seen that this is a very numerous group of raw materials, represented throughout the northern part of the IT excavation. Within 4 m from the hearth centre, there are over 4000 chips and flakes. The sector graph (fig. 61) shows very clearly that most repairing, resharpening or reworking took place to the southeast of the hearth. The remaining four sub-types are represented by only 59 flakes and chips within 4 m from

Table 5. IT, 1993 excavation. Raw materials within 4 m from the centre of the hearth inside the house in the northern part of the excavation.

Raw material groups	Chips	Chips: % per group	Non-chips	Total	Perc. of N
Chalcedony	3905	83.1	796	4701	64.8
Quartz	4	50.0	4	8	0.1
Rock crystal	826	81.9	183	1009	13.9
Killiaq	1094	71.4	438	1532	21.1
Total	5829	80.4	1421	7250	99.9

the hearth centre. One sub-type is present especially to the NE, outside the entrance; another to the northwest, near the meat cache (and inside it). The other artefacts are located close to the hearth, mainly to the west of it (fig. 62).

Rock crystal consists of two sub-types: 'clear' (transparent) and 'cracked'. These two sub-types have very different spatial distributions. The flakes and chips of cracked mountain crystal are present especially in the working area to the southeast of the hearth, just like the majority of the chalcedony artefacts (figs 63 and 64). Clear mountain crystal, on the other hand, has its main concentration to the north of the hearth, though there is a secondary concentration to the southeast (figs 65 and 66).

Killiaq can be subdivided into three sub-types. One of these, cream-coloured killiaq, once again shows a main concentration to the southeast of the hearth (figs 67 and 68). The two other sub-types are concentrated to the west of the hearth (light-grey killiaq: figs 69 and 70), and to the SSW of the hearth (dark-grey killiaq: figs 71 and 72), although they overlap somewhat in their

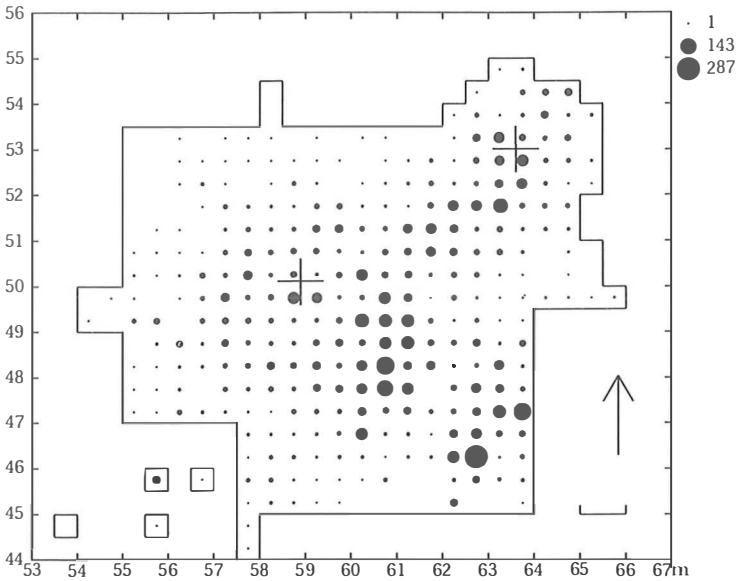

Fig. 60. IT. Density map of all chips and flakes of 10 sub-types of chalcedony: those having their richest sector in the SE or ESE. No classes, peripheral.

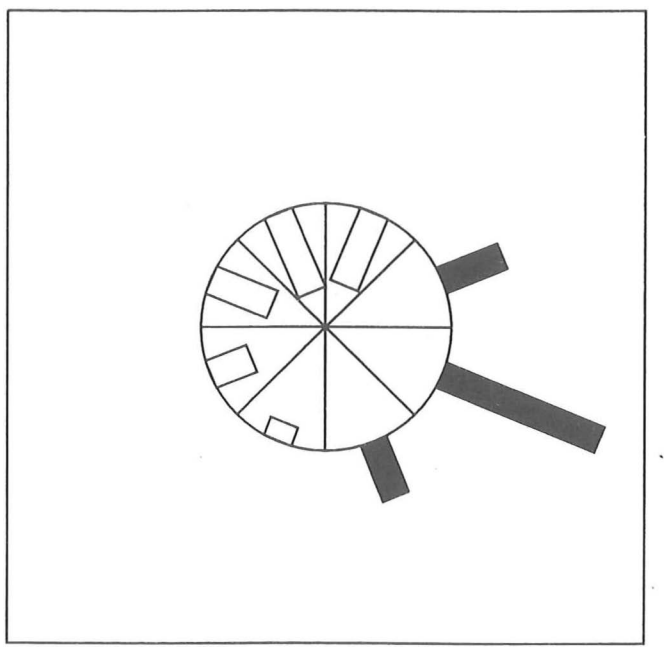

Fig. 61. IT. Sector graph of the chips and flakes of the same 10 sub-types of chalcedony as in fig. 60, within 4 m from the hearth centre. The centre of the sector wheel has the value zero; the circle represents the average number per sector (502.6). N = 4021.

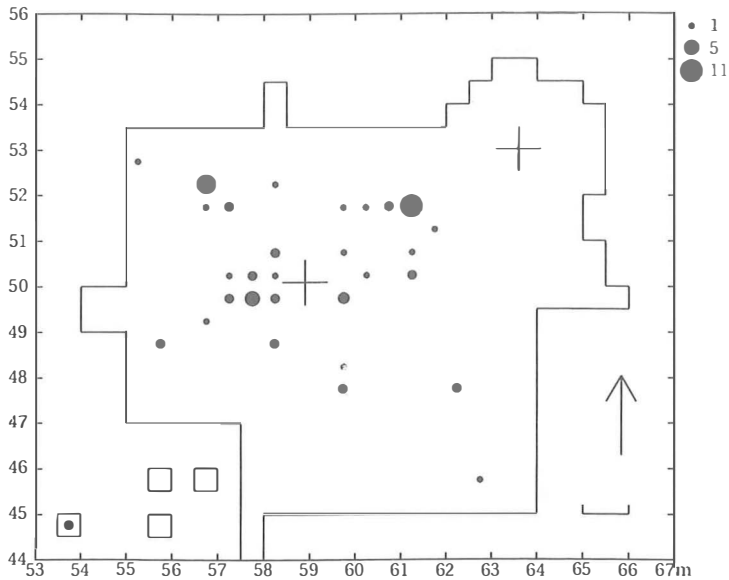

Fig. 62. IT. Density map of all chips and flakes of 4 subtypes of chalcedony: those having their richest sector not in the SE or ESE. No classes, peripheral.

distributions. The dark-grey killiaq presents us with a problem. On the basis of refitting (see fig. 58), the second author at first believed that this material might represent an occupation dating from after the occupation of the dwelling, because quite a few refitting lines cross its supposed wall, to the south of the hearth (compare with fig. 46). To investigate this matter more fully, a ring diagram for dark-grey killiaq (all artefacts) in sector 6 (SSW of the hearth) was produced: figure 73. Contrary to expectation, a clear wall effect can be seen, and the wall can be reconstructed in this sector at a distance of about 2.8 m from the hearth centre. Possibly, this state of affairs indicates a second opening in the wall, to the SSW of the hearth. The artefacts outside the wall might in that case reflect a small 'door dump' (or a 'window dump'?).

A special group of killiaq implements is constituted by pieces with a markedly rounded end. These mostly are broken tools, such as burin-like tools, which were re-used for some other purpose, which resulted in the rounding. The authors have experimented with this type of rounding at Lejre Research Centre, in the spring of 1995. The rounding is very similar to rounding observed on Late Palaeolithic, Mesolithic and Neolithic tools from various sites in northern Europe (see Johansen & Stapert, 1995). In the authors' opinion, the rounding was caused by use of these implements on pyrite, to make fire. Drawings of these tools, and microscope photos of their rounding, will be published elsewhere. Yet we may note that at both Dorset and Saqqaq sites in the Disko Bay area, pieces of pyrite have been found. Here, we will only present a map of these implements, eleven in total, at IT (fig. 74). It can be seen that these rounded killiaq implements cluster neatly near the three hearths thought to have been located inside dwellings. Several more possible fire-lighters have been found during the excavation at IT in the summer of 1995.

Finally, we present two density maps for soapstone fragments: one for fragments of bowl-shaped containers (fig. 75), the second for fragments of lamps (fig. 76). Interestingly, the lamp fragments mainly occur in the periphery of the dwelling in the northern part of IT, just inside the reconstructed walls. The bowl fragments, on the other hand, cluster near the hearths – just like the presumed fire-lighters. These bowls most probably served as cooking pots.

14. DISCUSSION AND SOME CONCLUSIONS

The main goal of this paper is to develop a technique for applying the ring and sector method in cases where most of the material was collected in grid cells of 50x50 cm. It is suggested that this can be done by constructing a theoretical file reflecting randomness. The observed ring (or sector) distributions are then compared with those displayed by the theoretical file, by subtracting the latter from the former (both expressed as percentages). This procedure not only takes care of incomplete rings, but also removes the 'pseudo-peaks' in ring (or sector) diagrams caused by the fact that the artefacts are given artificial coordinates in the middle of the grid cells. The 'pseudo-peaks' could also be removed by giving the artefacts random coordinates within the grid cells, instead of placing them at the centre. However, this would enlarge the mean estimation error (the maximum distance between the artificial locations and the real one's would then be 70 instead of 35 cm). Moreover, by applying random coordinates instead of the technique adopted in this paper, we would lose the advantage of correction for incomplete rings. Therefore, we believe that the procedure developed in this paper is to be

preferred for dealing with grid-cell data. It has to be stressed, however, that the use of grid cells larger than 50x50 cm precludes ring and sector analysis.

Using the technique described above, the ring distributions of the chips (flakes smaller than 1 cm) at the northern part of the IT site in Greenland were analysed, in eight sectors. On the basis of the obtained diagrams, the outline of the dwelling structure was reconstructed (fig. 46). The entrance was hypothesized to be in the ENE, because in that sector no clear 'barrier effect' in the ring diagram can be observed. Just outside the supposed entrance a small 'door dump' seems to be present. A much larger dump seems to be located a few metres to the southeast of the dwelling. Inside the dwelling, SE of the hearth, a large number of chips and flakes are found, of many different raw materials, in an area with a diameter of about 1.5 m. Here an activity area was located where tools were resharpened, reworked or repaired. The reconstructed outline of the dwelling, based on the ring and sector analysis, does not correspond completely with the excavators' expectations. For example, in the southeast the reconstructed wall is farther

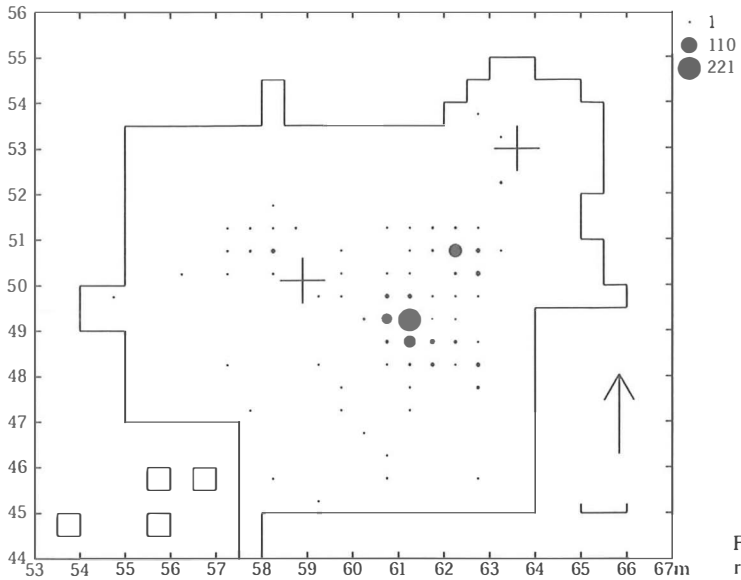

Fig. 63. IT. Density map of all chips and flakes of cracked rock crystal. No classes, peripheral.

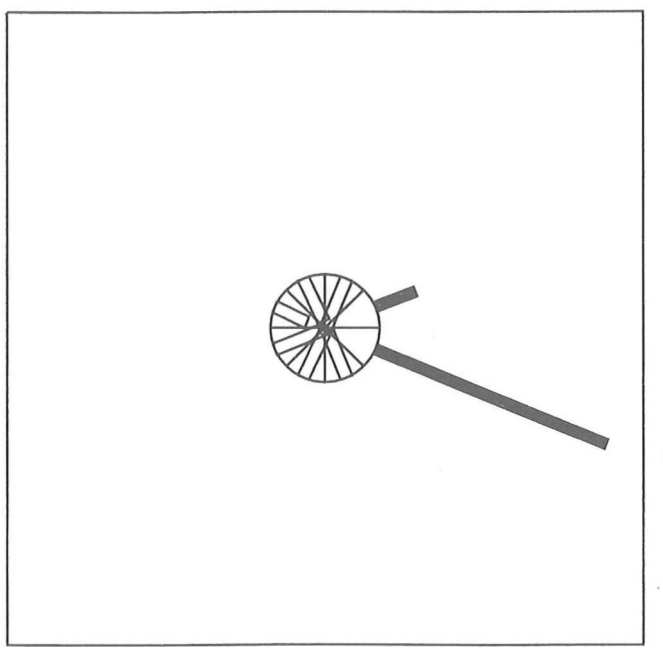

Fig. 64. IT. Sector graph of the chips and flakes of cracked rock crystal, within 4 m from the hearth centre. N = 574; mean: 71.7.

away from the hearth than anticipated on the basis of archaeologically visible features (larger stones considered to be structural elements). For the rest, however, the two approaches seem to be largely congruent in their conclusions.

It was hoped that analysis by the ring and sector method would also result in reliable hypotheses concerning the possibility of multiple occupations. However, we did not reach any definite conclusions regarding that matter. On the basis of refitting analysis, the second author has suggested that the concentration of dark-grey killiaq artefacts, south of the hearth, represents an activity of a later date than the occupation of the dwelling, because quite a few refitting lines cross the reconstructed wall of the dwelling. However, ring analysis reveals a clear 'wall effect' in this area by artefacts of dark-grey killiaq. One possible explanation is that there was a secondary opening in the wall here, with a door dump outside it. This seems to be all the more probable because the larger implements of this material cluster nicely around the hearth inside the dwelling. Ring and sector analysis and refitting analysis

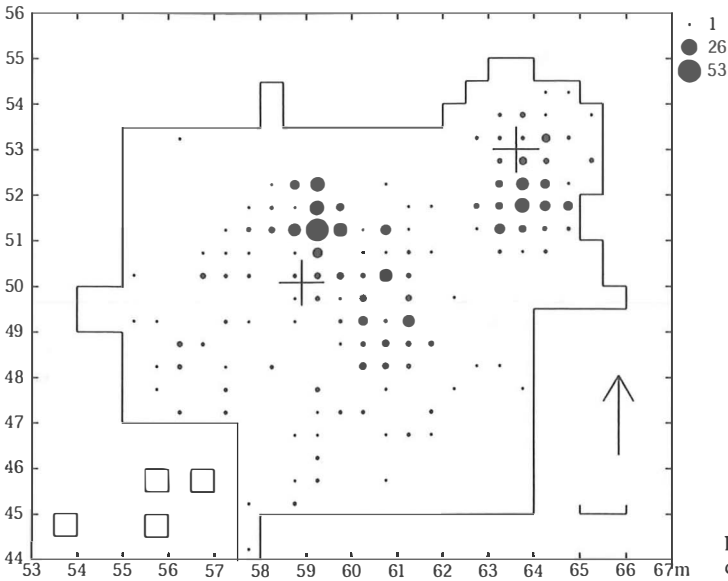

Fig. 65. IT. Density map of all chips and flakes of clear rock crystal. No classes, peripheral.

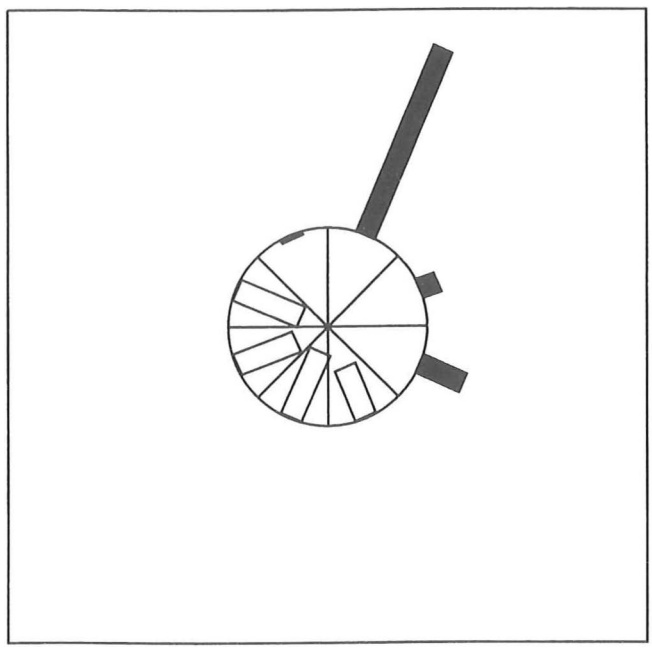

Fig. 66. IT. Sector graph of the chips and flakes of clear rock crystal, within 4 m from the hearth centre. N = 363; mean: 45.4.

appear to contradict each other in this matter. We want to state that this is most probably only an 'optical illusion', caused by the fact that they work with very different types of data. In reality, the two techniques neatly complement each other. Several other types of raw material also have deviating spatial distributions. For example, some types of chalcedony, represented by relatively few artefacts, show distributions radically different from most of the other raw materials. However, we have no way of investigating whether or not these materials represent later occupations.

The main conclusion of this paper is that analysis by the ring and sector method confirms the excavators' hypothesis that we are dealing with a dwelling structure in the northern part of the excavated area. On the basis of the work reported in this paper, this dwelling has an estimated inner diameter of 5-5.5 m, with the entrance in the ENE – facing the coast.

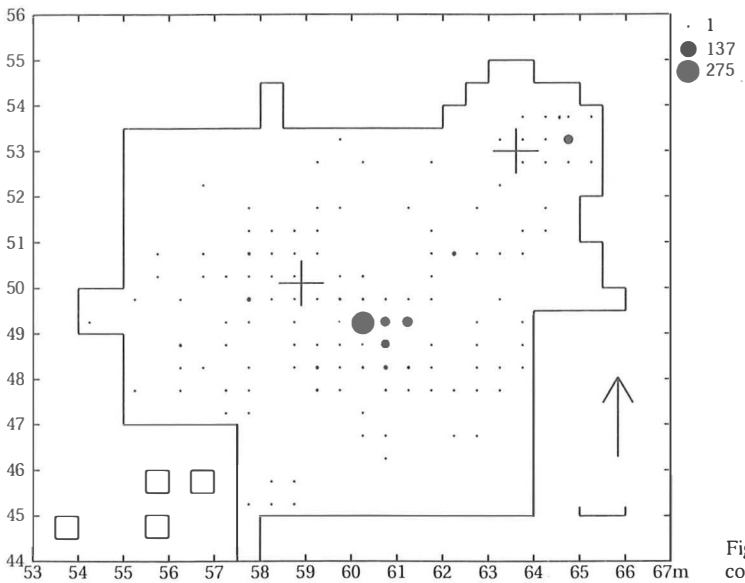

Fig. 67. IT. Density map of all chips and flakes of cream-coloured killiaq. No classes, peripheral.

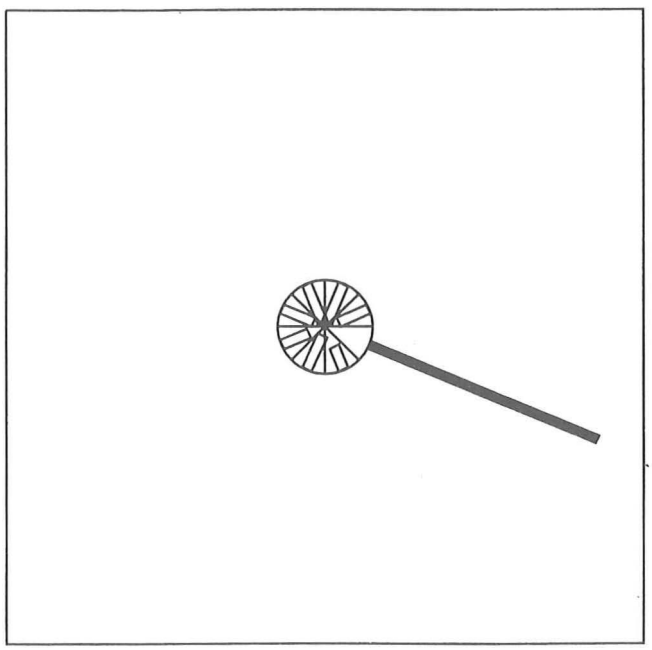

Fig. 68. IT. Sector graph of chips and flakes of cream-coloured killiaq, within 4 m from the hearth centre. N = 603; mean: 75.4.

15. ACKNOWLEDGEMENTS

We are grateful to the following persons and institutions for their contribution to the research reported in this text:

Gijsbert R. Boekschoten (Groningen) and Manfred Schweiger (Akili Software b.v., Groningen), for developing the R&S program, without which this paper could not have been written, and for stimulating discussions; Elisa Evaldsen (Aasiaat Museum) and Erik Brinch Petersen (Copenhagen), for permission to analyse spatial patterns of the IT site on Greenland. The first author also wishes to thank Brinch for the permission to stay and work at the Institut for Arkæologi og Etnologi for several months during the spring of 1995 – it was one of the most pleasant times of his life; Martin Street (Forschungsstelle Monrepos, Neuwied), for the opportunity to study the site of Andernach-Oben (we are preparing a paper devoted to that site), and for making several stays at Neuwied (by both of us) as pleasant as they were; Gerhard Bosinski (Forschungsstelle Monrepos, Neuwied), for his interest in the ring

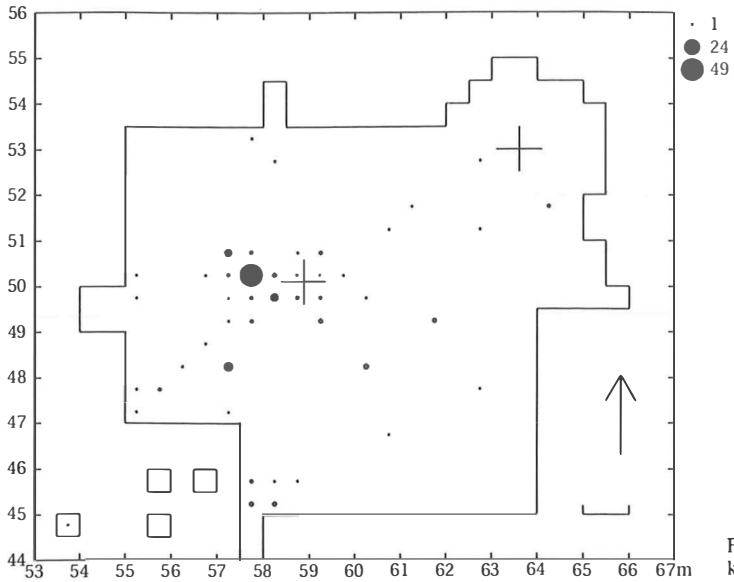

Fig. 69. IT. Density map of all chips and flakes of light-grey killiaq. No classes, peripheral.

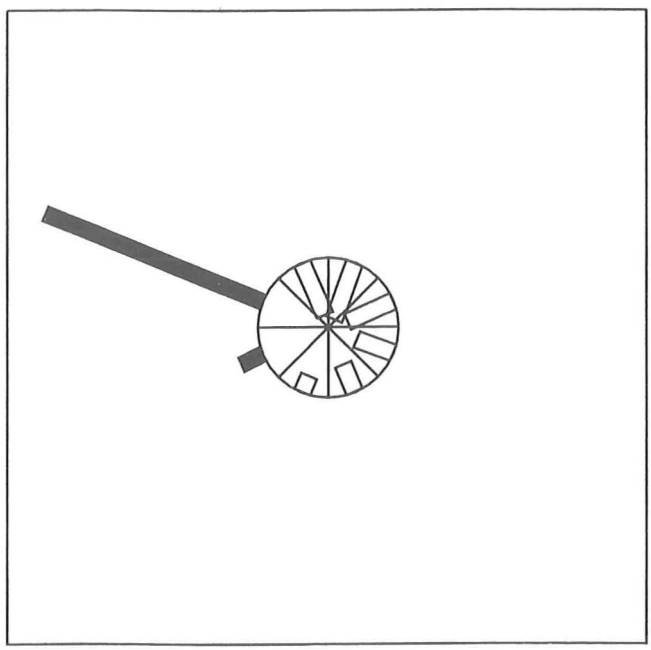

Fig. 70. IT. Sector graph of chips and flakes of light-grey killiaq, within 4 m from the hearth centre. N = 118; mean: 14.8.

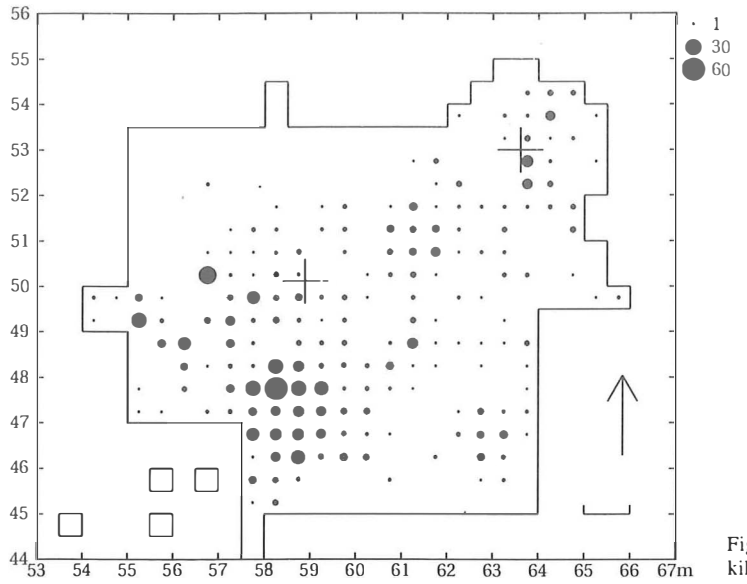

Fig. 71. IT. Density map of all chips and flakes of dark-grey killiaq. No classes, peripheral.

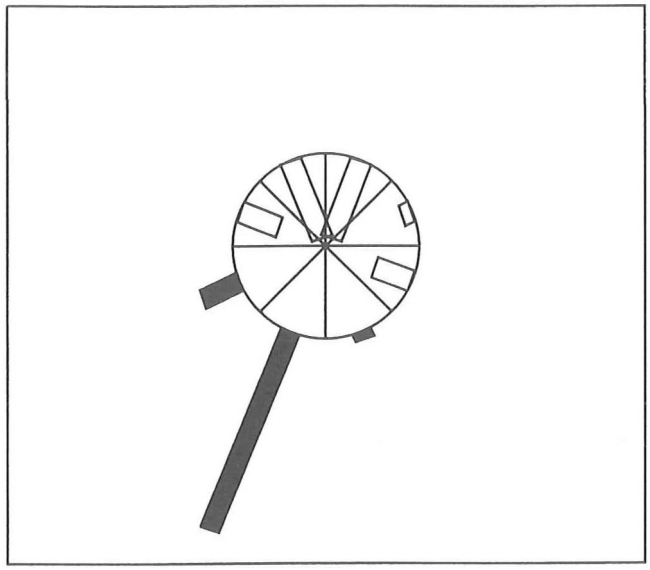

Fig. 72. IT. Sector graph of chips and flakes of dark-grey killiaq, within 4 m from the hearth centre. N = 769; mean: 96.1.

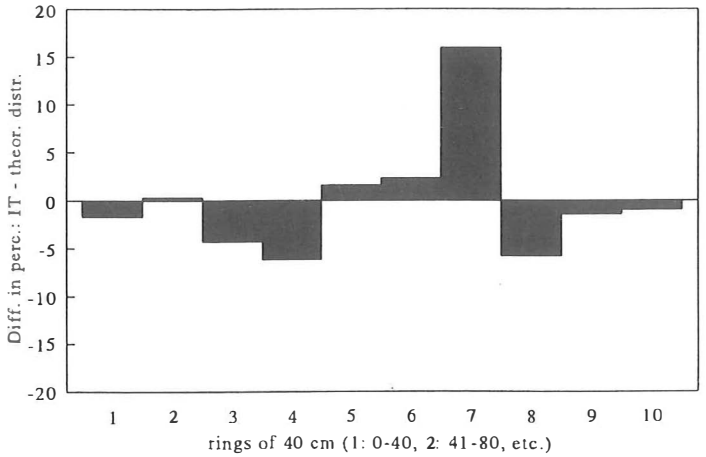

Fig. 73. IT. The ring distribution of all artefacts of dark-grey killiaq in sector 6 (SSW), after subtraction of the values of the theoretical distribution in the same sector, both expressed as percentages. Note the 'wall effect' in rings 7 and 8. N = 320.

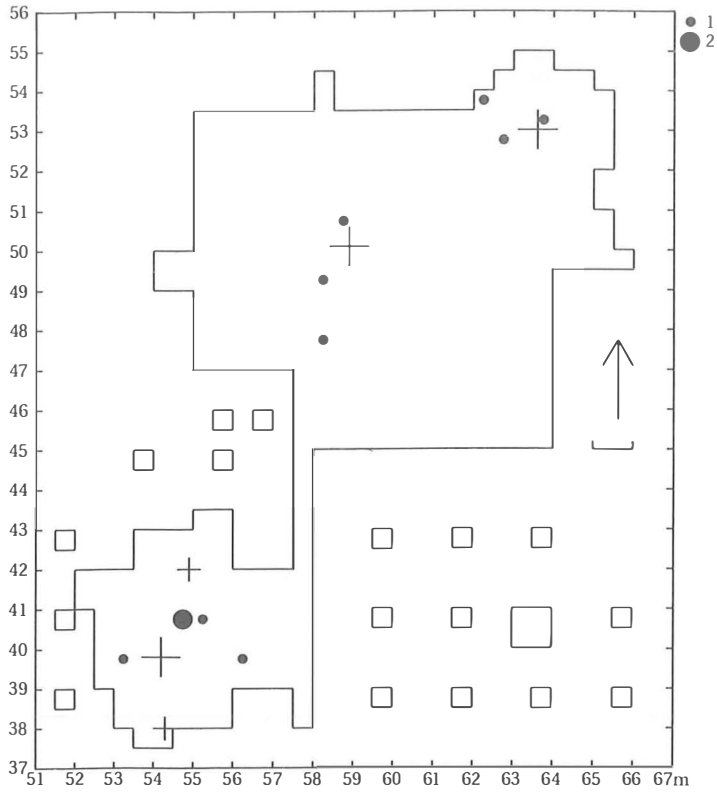

Fig. 74. IT. Density map of killiaq implements with a rounded end: fire-lighters? N = 11. Large crosses: hearths inside dwelling structures.

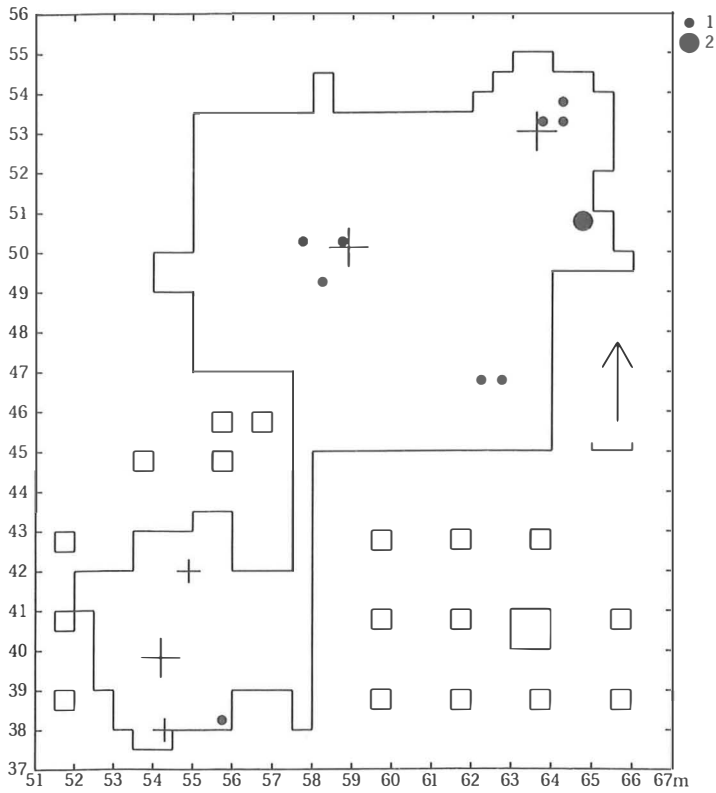

Fig. 75. IT. Density map of fragments of bowl-shaped containers made of soapstone. N = 11.

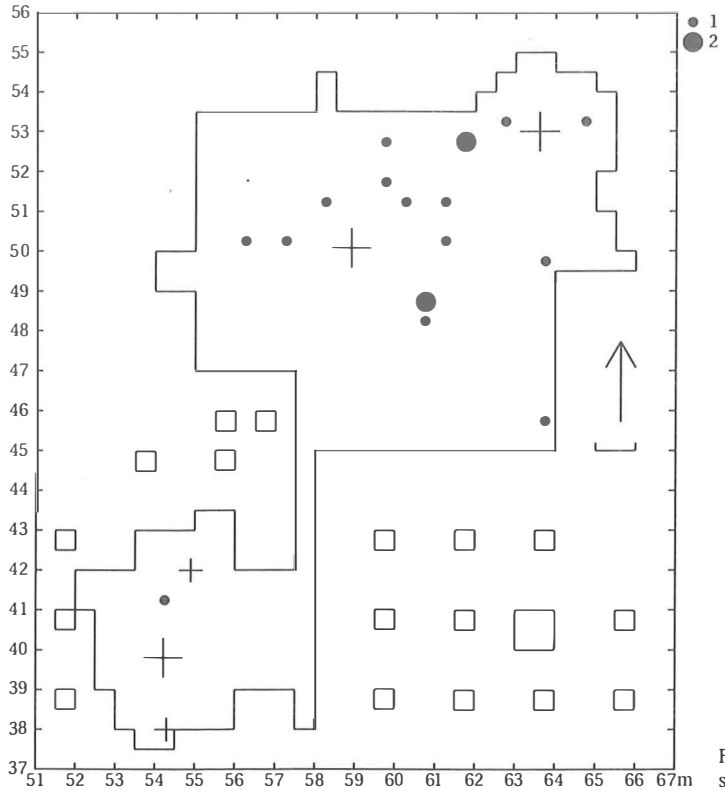

Fig. 76. IT. Density map of fragments of lamps made of soapstone. N = 18.

and sector method and his support during its development, and for his permission to work with the data of the site of Gönnersdorf; Sabine Eickhoff (Brandenburg), for kindly making available her data concerning Gönnersdorf Concentration II; Marc de Bie (Louvain), for critically reading a first draft; Per Enggærd Pedersen (National Museum, Copenhagen), for his help in starting up the IT project in the spring of 1995; Groningen Institute of Archaeology, especially Reinder Reinders, for giving the first author leave to participate in this research project – which entailed a three-month absence from the institute; Xandra Bardet (Groningen), for expertly correcting our English text.

16. REFERENCES

BLANKHOLM, H.P., 1991/1992. Rings, sectors and Barmose I: a reply to Stapert. *Palaeohistoria* 33/34, pp. 53-57.

BOEKSCHOTEN, G.R. & D. STAPERT, 1993. Rings & Sectors: a computer package for spatial analysis; with examples from Oldeholtwolde and Gönnersdorf. *Helinium* 33, pp. 20-35.

BOEKSCHOTEN, G.R. & D. STAPERT, in press. A new tool for spatial analysis: 'Rings & Sectors 3.1 plus Density Analysis and Tracelines. Paper presented at the 23ed CAA Conference, 'Interfacing the Past'; Leiden 31 March – 2 April 1995.

BOEKSCHOTEN, G.R., M.M. SCHWEIGER & D. STAPERT, 1994. *Manual for the computer package 'Rings & Sectors 2.0 plus Density Analysis'*. Akili Software B.V., Groningen.

BOSINSKI, G., 1979. *Die Ausgrabungen in Gönnersdorf 1968-1976 und die Siedlungsbefunde der Grabung 1968.* (= Gönnersdorf Band 3). Franz Steiner, Wiesbaden.

BUSCHKÄMPER, TH., 1993. Die Befunde im Südwestteil der Gönnersdorfer Grabungsfläche. Magisterarbeit, University of Cologne.

CZIESLA, E., 1990. *Siedlungsdynamik auf steinzeitlichen Fundplätzen; methodische Aspekte zur Analyse latenter Strukturen.* (= Studies in Modern Archaeology, Vol. 2). Holos, Bonn.

DE BIE, M., 1993. Compte-rendu of: Stapert, 1992. *Helinium* 33, pp. 138-141.

EVALDSEN, E. & E. BRINCH PETERSEN, 1995. The Museum of Aasiaat: Ikkarlussuup Tima; Excavation of an Early Dorset site in Disko Bay, Western Greenland. *Prince of Wales, Northern Heritage Centre; Archaeology Report* 16, pp. 46-50.

FLETCHER, M. & G.R. LOCK, 1991. *Digging numbers; elementary statistics for archaeologists* (= Oxford University Committee for Archaeology, Monograph 33). Oxford.

FRANKEN, E. & S. VEIL, 1983. *Die Steinartefakte von Gönnersdorf* (= Gönnersdorf Band 7). Franz Steiner, Wiesbaden.

JOHANSEN, L. & D. STAPERT, 1995. 'Vuur-stenen' in het late Paleolithicum. *Paleo-aktueel* 6, pp. 12-15.

SCHMIDER, B. (ed.), 1992. *Marsangy; un campement des derniers chasseurs magdaléniens, sur les bords de l'Yonne* (= Etudes et Recherches Archéologiques de l'Université de Liège vol. 55). Liège.

STAPERT, D., 1989. The ring and sector method: intrasite spatial analysis of Stone Age sites, with special reference to Pincevent. *Palaeohistoria* 31, pp. 1-57.

STAPERT, D., 1990. Within the tent or outside? Spatial patterns in Late Palaeolithic sites. *Helinium* 30, pp. 14-35.

STAPERT, D., 1992. Rings and sectors: intrasite spatial analysis of Stone Age sites. Thesis, Groningen University.

STAPERT, D. & TH. TERBERGER, 1989. Gönnersdorf Concentration III: investigating the possibility of multiple occupations. *Palaeohistoria* 31, pp. 59-95.